SUPPLEMENTARY MATERIALS

Clinical efficacy of ONC201 in H3K27M-mutant diffuse midline gliomas is driven by disruption of integrated metabolic and epigenetic pathways

Supplementary Data

Data S1. Protocol for NCT03416530, ONC201-014: ONC201 in Newly Diagnosed Diffuse Intrinsic Pontine Glioma and Recurrent/Refractory Pediatric H3K27M Gliomas.

Data S2. Protocol for NCT03134131, ONC201-018: Expanded Access to ONC201 for Patients with H3K27M-mutant and/or Midline High Grade Gliomas.

Supplementary Tables

Table S1. Baseline characteristics of ONC201-treated H3K27M-DMG patients included in analysis.

Table S2. Individual patients with H3K27M-mutant DMG treated with ONC201.

Table S3. Individual cases from historical control datasets.

Table S4. Summary of historical control datasets.

Table S5: VST-transformed gene expression values for all samples and protein-coding genes.

Table S6: Radiographic response *versus* gene expression Spearman's correlation coefficient for all protein-coding genes.

Table S7: GSEA of genes associated with positive or negative correlation with radiographic response to ONC201 treatment.

Table S8: Expression values, Spearman's correlation coefficient, and GSEA of genes associated with positive or negative correlation with radiographic response to ONC201 treatment.

Table S9: Upregulated and downregulated genes in DIPG007 cells treated with ONC201 *versus* vehicle.

Table S10: Upregulated and downregulated metabolites in DIPG007 cells treated with ONC201 *versus* vehicle.

Table S11: Volcano plot of differentially expressed genes in DIPG007 cells treated with ONC201 *versus* vehicle.

Table S12: Results of pathway impact analysis after performing integrated RNA-seq and metabolomics analysis using MetaboAnalyst.

Table S13: GSEA analysis of genes with significantly lower chromatin accessibility at promoters and enhancers and reduced gene expression in DIPG007 cells treated with ONC201 *versus* vehicle.

Table S14: GSEA analysis of genes with significantly lower H3K27ac at promoters and enhancers and reduced gene expression in DIPG007 cells treated with ONC201 *versus* vehicle.

Table S15: GSEA analysis of genes with significantly increased H3K27me3 in ONC201-treated *versus* untreated patients.

Table S16. ONC201 dosage chart for patients younger than 18 years of age.

Supplementary Figures with Legends

Fig. S1. Selection method for planned efficacy analysis of ONC201 in patients with H3K27M-DMG.

Fig. S2. Progression-free survival from diagnosis of trial patients with non-recurrent H3K27M-DMG treated with ONC201.

Fig. S3. Swimmers' plot of ONC201 response by recurrence status, tumor location, and ONC201 trial.

Fig. S4. ONC201 efficacy is independent of TP53 mutation status and chromosomal instability.

Fig. S5. Cox proportional hazard regression to assess the effect of ONC201 after adjusting for confounders.

Fig. S6. Survival of patients with H3K27M-DMG treated with ONC201 *versus* ONC201-untreated historical controls.

Fig. S7. Survival of patients with H3K27M-DMG treated with ONC201 *versus* ONC201-untreated patients (PNOC003 or HERBY Phase II trials).

Fig. S8. Molecular attributes of patients with H3K27M-DMG treated with ONC201.

Fig. S9: Survival of H3K27M-DMG mice models treated with ONC201.

Fig. S10. Integrative analysis of *in vitro* and human tumor metabolic gene expression in response to ONC201.

Fig. S11. ONC201-mediated L2HG production increases H3K27me3 in H3K27M-DMG cells.

Fig. S12. ONC201-induced increase in H3K27me3 is mediated by lactate dehydrogenase.

Fig. S13. ONC201 alters genomic chromatin accessibility and H3K27ac distribution in H3K27M-DMG cells.

Fig. S14. ONC201 increases global H3K27me3 in patient samples.

Fig. S15. ONC201 does not cause hypermethylation leading to a glioma CpG island methylator phenotype.

Fig. S1. Selection method for planned efficacy analysis of ONC201 in patients with H3K27M-DMG.

All patients enrolled in completed arms of ONC201-014 at the recommended phase 2 dose (RP2D) and all patients enrolled in ONC201-018 with thalamic and brainstem tumors treated with ONC201 were screened. One hundred-and-eight total patients with thalamic and brainstem DMG were screened. Thirty-six total patients were excluded (5 patients from ONC201-014 and 31 patients from ONC201-018) due to unconfirmed H3K27M mutation status, inability to verify follow-up date at time of analysis, or inability to satisfy requirement for recurrent or non-recurrent disease after irradiation. Seventy-one total patients met the inclusion criteria and were included in final analysis, of which 35 enrolled following irradiation prior to recurrence while 36 enrolled with recurrent disease.

FIGURE S1

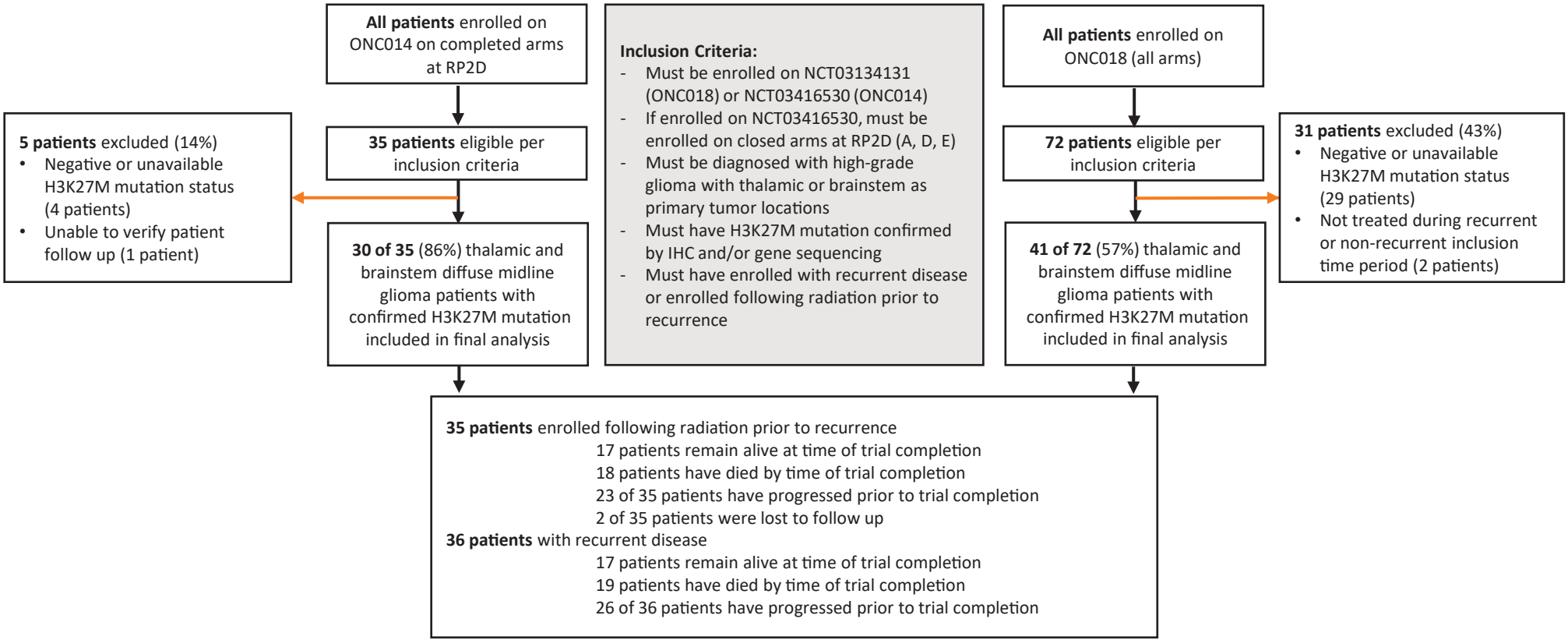
All patients enrolled on ONC014 on completed arms at RP2D
35 patients eligible per inclusion criteria
30 of 35 (86%) thalamic and brainstem diffuse midline glioma patients with confirmed H3K27M mutation included in final analysis
5 patients excluded (14%)
• Negative or unavailable H3K27M mutation status (4 patients)
• Unable to verify patient follow up (1 patient)
Inclusion Criteria:
- Must be enrolled on NCT03134131 (ONC018) or NCT03416530 (ONC014)
- If enrolled on NCT03416530, must be enrolled on closed arms at RP2D (A, D, E)
- Must be diagnosed with high-grade glioma with thalamic or brainstem as primary tumor locations
- Must have H3K27M mutation confirmed by IHC and/or gene sequencing
- Must have enrolled with recurrent disease or enrolled following radiation prior to recurrence
All patients enrolled on ONC018 (all arms)
72 patients eligible per inclusion criteria
41 of 72 (57%) thalamic and brainstem diffuse midline glioma patients with confirmed H3K27M mutation included in final analysis
31 patients excluded (43%)
• Negative or unavailable H3K27M mutation status (29 patients)
• Not treated during recurrent or non-recurrent inclusion time period (2 patients)
35 patients enrolled following radiation prior to recurrence
17 patients remain alive at time of trial completion
18 patients have died by time of trial completion
23 of 35 patients have progressed prior to trial completion
2 of 35 patients were lost to follow up
36 patients with recurrent disease
17 patients remain alive at time of trial completion
19 patients have died by time of trial completion
26 of 36 patients have progressed prior to trial completion

Fig. S2. Progression-free survival from diagnosis of trial patients with non-recurrent H3K27M-DMG treated with ONC201.

Kaplan-Meier curve (Y-axis, % PFS; X-axis, time in months) showing PFS from diagnosis for non-recurrent H3K27M-DMG patients treated with ONC201 by study (ONC201-014, blue, n=24; ONC201-018, light blue, n=11; and ONC201-014/018 combined, orange, n=35).

FIGURE S2

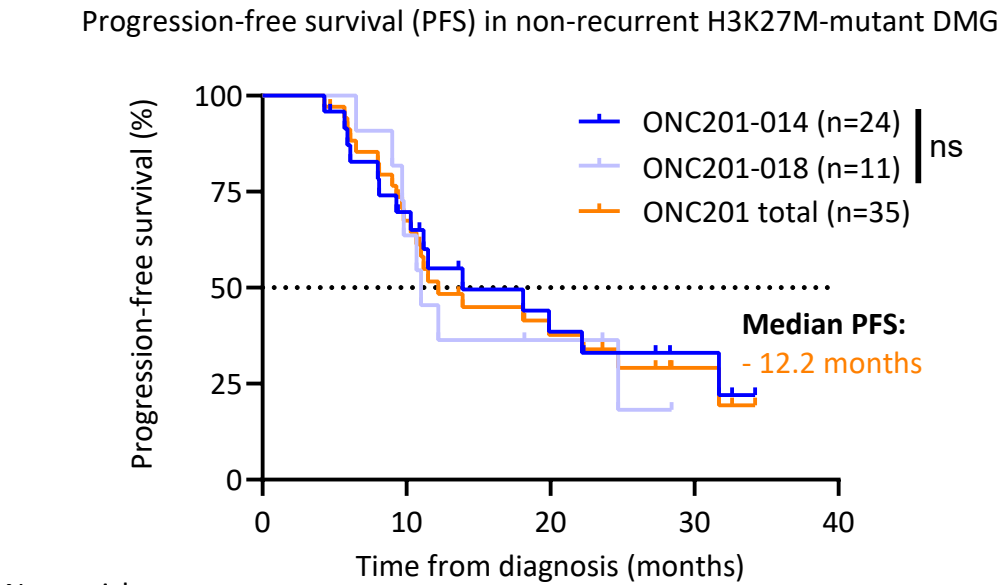

No. at risk:					
ONC201-014	24	15	7	3	0
ONC201-018	11	7	3	0	0
ONC201 total	35	22	10	3	0

Fig. S3. Swimmers' plot of ONC201 response by recurrence status, tumor location, and ONC201 trial.

Detailed treatment information for each patient (Y-axis) segregated by (top) recurrence status, (middle) tumor location, and (bottom) ONC201 trial: yellow bar = months from starting ONC201 treatment; gray bar = radiotherapy; blue bar = treatment to end or screen; white bar = time off treatment with survival; black triangle = progression; red circle = death; black arrow = alive at end of analysis.

FIGURE S3

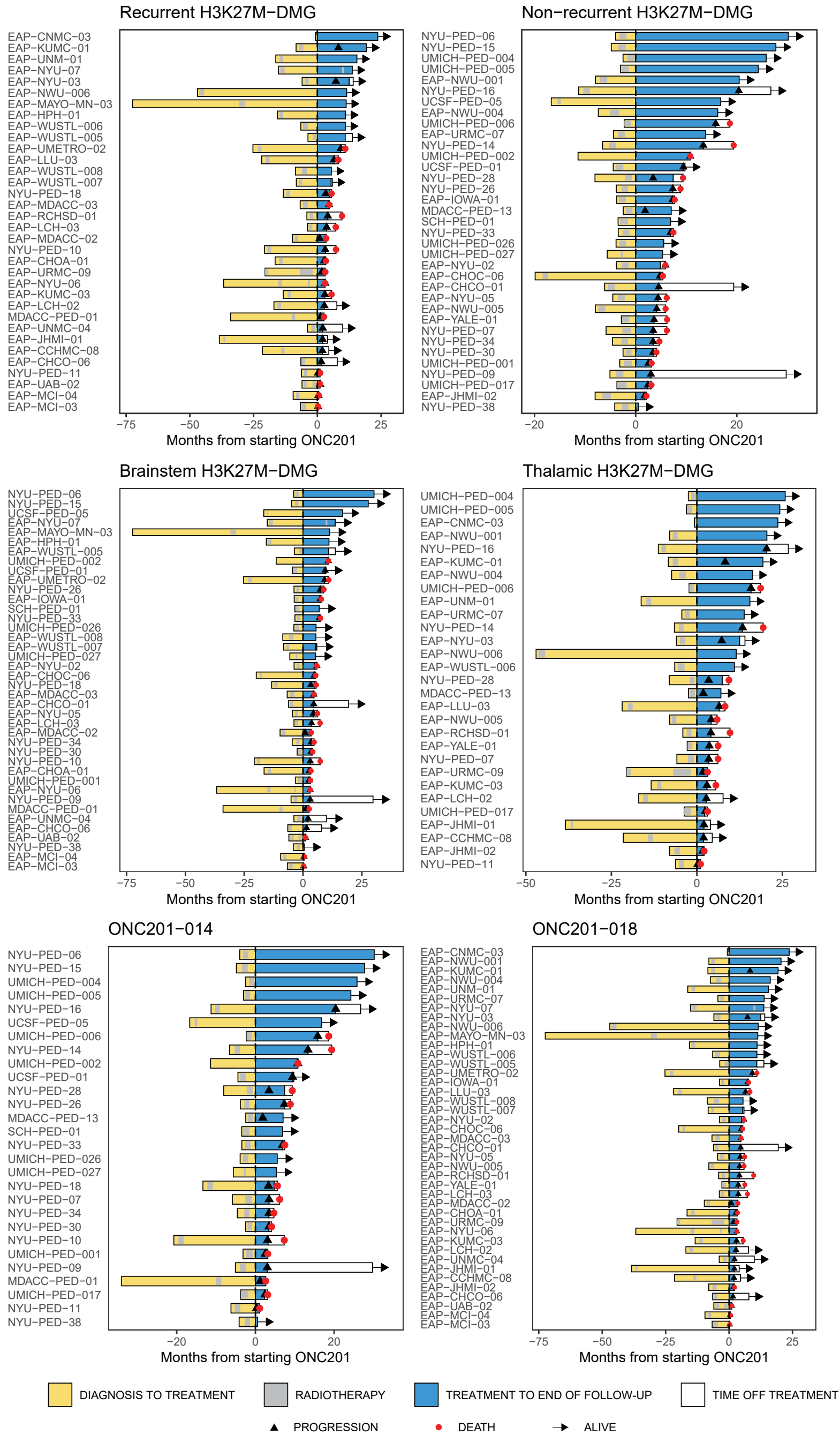
Recurrent H3K27M−DMG
EAP−CNMC−03
EAP−KUMC−01
EAP−UNM−01
EAP−NYU−07
EAP−NYU−03
EAP−NWU−006
EAP−MAYO−MN−03
EAP−HPH−01
EAP−WUSTL−006
EAP−WUSTL−005
EAP−UMETRO−02
EAP−LLU−03
EAP−WUSTL−008
EAP−WUSTL−007
NYU−PED−18
EAP−MDACC−03
EAP−RCHSD−01
EAP−LCH−03
EAP−MDACC−02
NYU−PED−10
EAP−CHOA−01
EAP−URMC−09
EAP−NYU−06
EAP−KUMC−03
EAP−LCH−02
MDACC−PED−01
EAP−UNMC−04
EAP−JHMI−01
EAP−CCHMC−08
EAP−CHCO−06
NYU−PED−11
EAP−UAB−02
EAP−MCI−04
EAP−MCI−03
−75
−50
−25
0
25
Months from starting ONC201
Non−recurrent H3K27M−DMG
NYU−PED−06
NYU−PED−15
UMICH−PED−004
UMICH−PED−005
EAP−NWU−001
NYU−PED−16
UCSF−PED−05
EAP−NWU−004
UMICH−PED−006
EAP−URMC−07
NYU−PED−14
UMICH−PED−002
UCSF−PED−01
NYU−PED−28
NYU−PED−26
EAP−IOWA−01
MDACC−PED−13
SCH−PED−01
NYU−PED−33
UMICH−PED−026
UMICH−PED−027
EAP−NYU−02
EAP−CHOC−06
EAP−CHCO−01
EAP−NYU−05
EAP−NWU−005
EAP−YALE−01
NYU−PED−07
NYU−PED−34
NYU−PED−30
UMICH−PED−001
NYU−PED−09
UMICH−PED−017
EAP−JHMI−02
NYU−PED−38
−20
0
20
Months from starting ONC201
Brainstem H3K27M−DMG
NYU−PED−06
NYU−PED−15
UCSF−PED−05
EAP−NYU−07
EAP−MAYO−MN−03
EAP−HPH−01
EAP−WUSTL−005
UMICH−PED−002
UCSF−PED−01
EAP−UMETRO−02
NYU−PED−26
EAP−IOWA−01
SCH−PED−01
NYU−PED−33
UMICH−PED−026
EAP−WUSTL−008
EAP−WUSTL−007
UMICH−PED−027
EAP−NYU−02
EAP−CHOC−06
NYU−PED−18
EAP−MDACC−03
EAP−CHCO−01
EAP−NYU−05
EAP−LCH−03
EAP−MDACC−02
NYU−PED−34
NYU−PED−30
NYU−PED−10
EAP−CHOA−01
UMICH−PED−001
EAP−NYU−06
NYU−PED−09
MDACC−PED−01
EAP−UNMC−04
EAP−CHCO−06
EAP−UAB−02
NYU−PED−38
EAP−MCI−04
EAP−MCI−03
−75
−50
−25
0
25
Months from starting ONC201
Thalamic H3K27M−DMG
UMICH−PED−004
UMICH−PED−005
EAP−CNMC−03
EAP−NWU−001
NYU−PED−16
EAP−KUMC−01
EAP−NWU−004
UMICH−PED−006
EAP−UNM−01
EAP−URMC−07
NYU−PED−14
EAP−NYU−03
EAP−NWU−006
EAP−WUSTL−006
NYU−PED−28
MDACC−PED−13
EAP−LLU−03
EAP−NWU−005
EAP−RCHSD−01
EAP−YALE−01
NYU−PED−07
EAP−URMC−09
EAP−KUMC−03
EAP−LCH−02
UMICH−PED−017
EAP−JHMI−01
EAP−CCHMC−08
EAP−JHMI−02
NYU−PED−11
−50
−25
0
25
Months from starting ONC201
ONC201−014
NYU−PED−06
NYU−PED−15
UMICH−PED−004
UMICH−PED−005
NYU−PED−16
UCSF−PED−05
UMICH−PED−006
NYU−PED−14
UMICH−PED−002
UCSF−PED−01
NYU−PED−28
NYU−PED−26
MDACC−PED−13
SCH−PED−01
NYU−PED−33
UMICH−PED−026
UMICH−PED−027
NYU−PED−18
NYU−PED−07
NYU−PED−34
NYU−PED−30
NYU−PED−10
UMICH−PED−001
NYU−PED−09
MDACC−PED−01
UMICH−PED−017
NYU−PED−11
NYU−PED−38
−20
0
20
Months from starting ONC201
ONC201−018
EAP−CNMC−03
EAP−NWU−001
EAP−KUMC−01
EAP−NWU−004
EAP−UNM−01
EAP−URMC−07
EAP−NYU−07
EAP−NYU−03
EAP−NWU−006
EAP−MAYO−MN−03
EAP−HPH−01
EAP−WUSTL−006
EAP−WUSTL−005
EAP−UMETRO−02
EAP−IOWA−01
EAP−LLU−03
EAP−WUSTL−008
EAP−WUSTL−007
EAP−NYU−02
EAP−CHOC−06
EAP−MDACC−03
EAP−CHCO−01
EAP−NYU−05
EAP−NWU−005
EAP−RCHSD−01
EAP−YALE−01
EAP−LCH−03
EAP−MDACC−02
EAP−CHOA−01
EAP−URMC−09
EAP−NYU−06
EAP−KUMC−03
EAP−LCH−02
EAP−UNMC−04
EAP−JHMI−01
EAP−CCHMC−08
EAP−JHMI−02
EAP−CHCO−06
EAP−UAB−02
EAP−MCI−04
EAP−MCI−03
−75
−50
−25
0
25
Months from starting ONC201
DIAGNOSIS TO TREATMENT
RADIOTHERAPY
TREATMENT TO END OF FOLLOW-UP
TIME OFF TREATMENT
PROGRESSION
DEATH
ALIVE

Fig. S4. ONC201 efficacy is independent of TP53 mutation status and chromosomal instability.

(**A**) Bar graph showing percentage of responders (n=10) and non-responders (n=10) bearing (left) *TP53* mutations and/or (right) chromosomal instability (CIN).

(**B**) Box plots demonstrating association of *TP53* mutation status with (left) increased CIN ($p<0.0001$) and (middle) CIN loss scores ($p<0.0001$) but not with (right) CIN gain scores ($p=0.09$).

(**C-D**) Kaplan-Meier curves comparing (**C**) OS from diagnosis and (**D**) PFS from diagnosis for 6 patients with non-recurrent H3K27M-DMG treated with ONC201 from the ONC201-014 arm stratified by *TP53* status (yellow = wildtype; blue = mutant).

(**E-F**) Kaplan-Meier curves comparing (**E**) OS from diagnosis and (**F**) PFS from diagnosis for 6 patients with non-recurrent H3K27M-DMG treated with ONC201 from the ONC201-014 arm stratified by CIN status (yellow = low; blue = high).

FIGURE S4

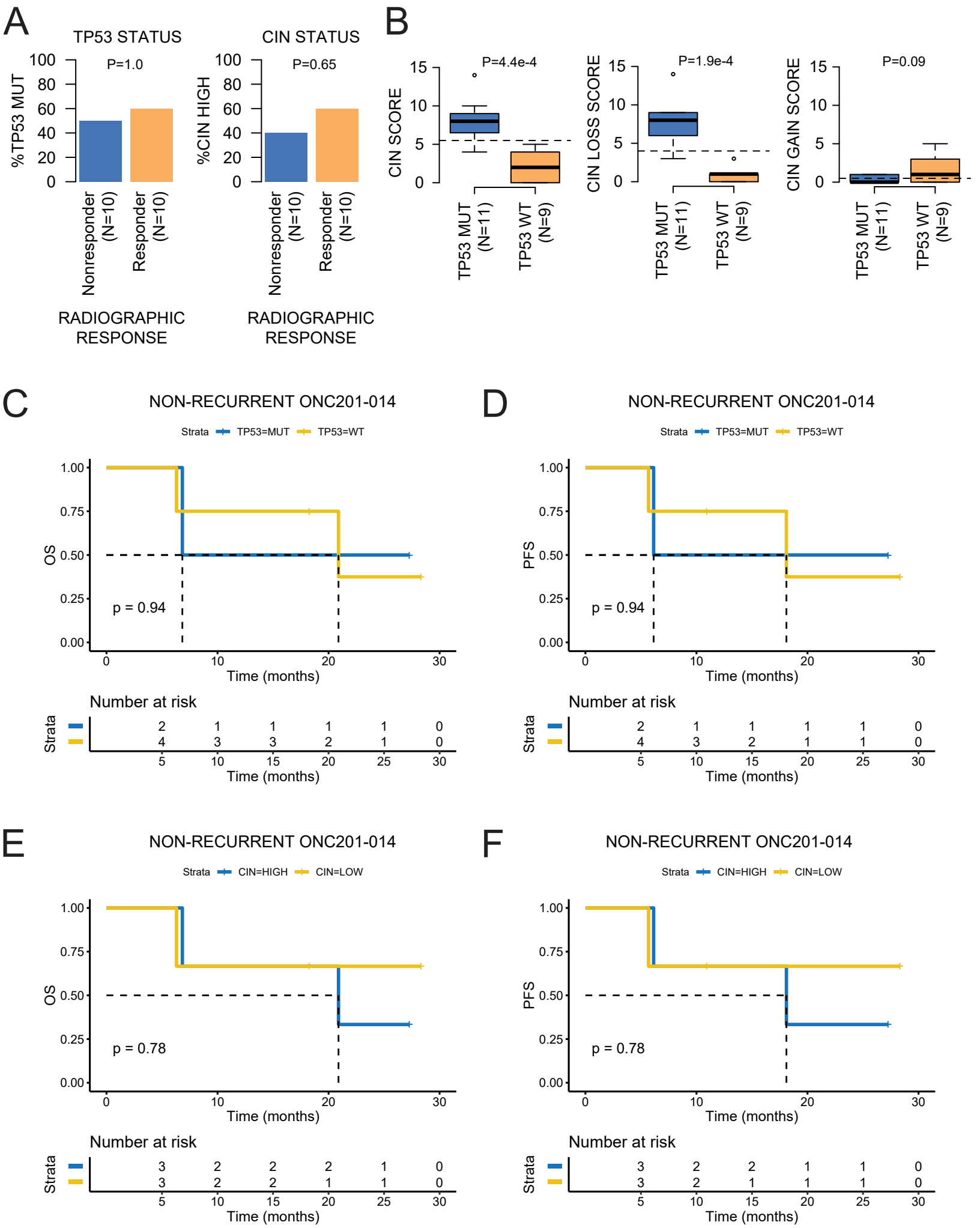
A
TP53 STATUS
P=1.0
%TP53 MUT
Nonresponder (N=10)
Responder (N=10)
RADIOGRAPHIC RESPONSE
CIN STATUS
P=0.65
%CIN HIGH
B
P=4.4e-4
CIN SCORE
TP53 MUT (N=11)
TP53 WT (N=9)
P=1.9e-4
CIN LOSS SCORE
P=0.09
CIN GAIN SCORE
C
NON-RECURRENT ONC201-014
Strata TP53=MUT TP53=WT
OS
p = 0.94
Time (months)
Number at risk
D
PFS
E
CIN=HIGH CIN=LOW
p = 0.78
F

Fig. S5. Cox proportional hazard regression to assess the effect of ONC201 after adjusting for confounders.

(**A**) Cox proportional hazard regression analysis (X-axis, HR = hazard ratio) of OS was performed to assess for possible confounders (Y-axis, gender, age, and tumor location) between ONC201-treated or untreated (historical dataset, see **Supplementary Fig. S6**) non-recurrent H3K27M-DMG (larger HR = larger effect of confounder).

(**B**) Cox proportional hazard regression analysis (X-axis, HR = hazard ratio) of OS after excluding early deaths from historical cohort was performed to assess for possible confounders (Y-axis, gender, age, and tumor location) between ONC201-treated or untreated (historical dataset, see **Supplementary Fig. S6**) non-recurrent H3K27M-DMG (larger HR = larger effect of confounder).

FIGURE S5

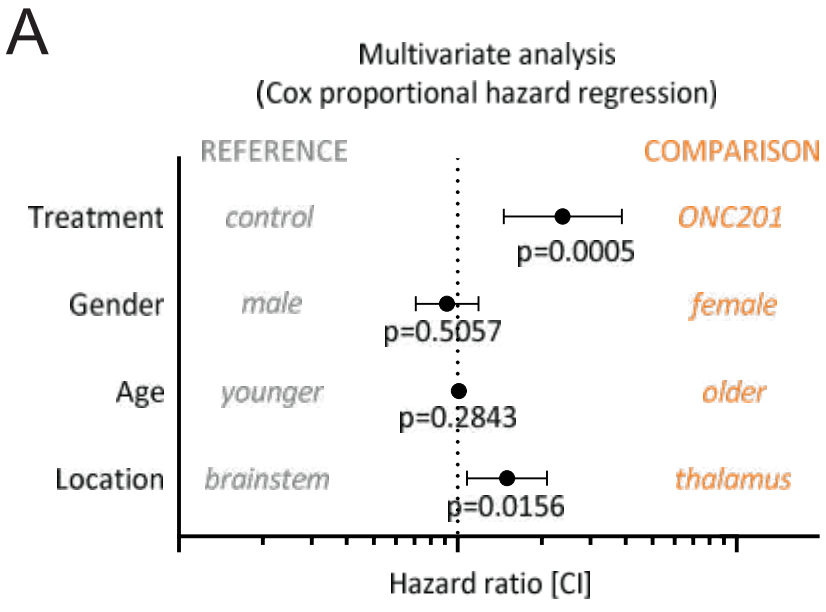
A
Multivariate analysis
(Cox proportional hazard regression)
REFERENCE
COMPARISON
Treatment
control
ONC201
p=0.0005
Gender
male
female
p=0.5057
Age
younger
older
p=0.2843
Location
brainstem
thalamus
p=0.0156
Hazard ratio [CI]

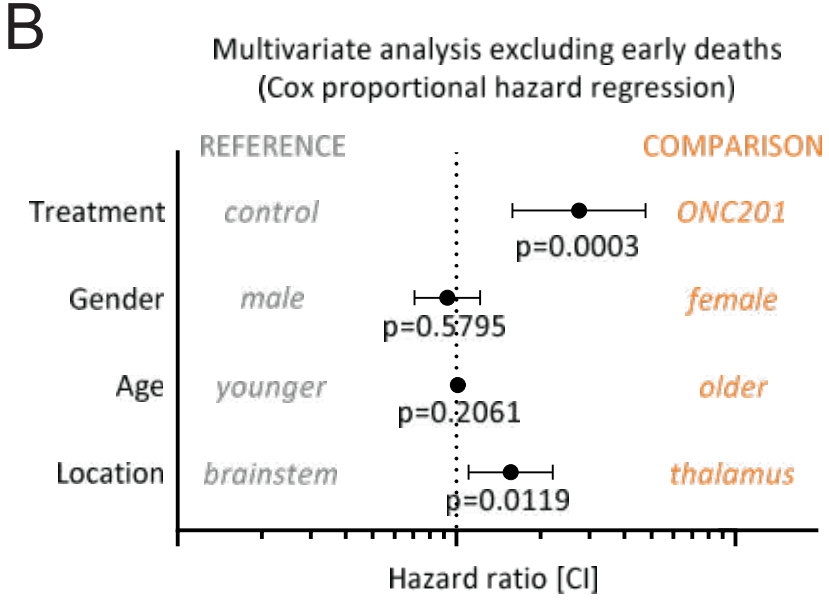
B
Multivariate analysis excluding early deaths
(Cox proportional hazard regression)
REFERENCE
COMPARISON
Treatment
control
ONC201
p=0.0003
Gender
male
female
p=0.5795
Age
younger
older
p=0.2061
Location
brainstem
thalamus
p=0.0119
Hazard ratio [CI]

Fig. S6. Survival of patients with H3K27M-DMG treated with ONC201 *versus* ONC201-untreated historical controls.

(**A**) Kaplan-Meier curve (Y-axis, % overall survival; X-axis, time in months) comparing OS from diagnosis for 35 patients with non-recurrent H3K27M-DMG treated with ONC201 from both studies (n=35, orange, median OS = 21.7 months) *versus* OS in historical controls (n=274, gray, median OS = 12 months). Historical controls derived from Pratt *et al.* (2018) *Acta Neuropathologica*.

(**B**) Kaplan-Meier curve (Y-axis, % overall survival; X-axis, time in months) comparing OS from recurrence for 36 patients with recurrent H3K27M-DMG treated with ONC201 from both studies (n=36, orange, median OS = 9.3 months) *versus* OS in historical controls (n=99, gray, median OS = 8.1 months). Historical controls derived from Castel *et al.* (2018) *Acta Neuropathol Commun*, Lobon-Iglesias *et al.* (2018) *J Neuro Oncology*, and an unpublished cohort from the Gustave Roussy Institute, France.

(**C**) Kaplan-Meier curve (Y-axis, % overall survival; X-axis time in months) comparing OS from diagnosis for 35 patients with non-recurrent H3K27M-DMG treated with ONC201 from both studies *versus* OS in historical controls by anatomic location (thalamus or brainstem). ONC201-treated thalamic H3K27M-DMG (n=15, orange, median OS = 20.9 months) *versus* historical thalamic H3K27M-DMG (n=68, gray, median OS = 14.5 months). ONC201-treated brainstem H3K27M-DMG (n= 20, blue, median OS = 21.7 months) *versus* historical brainstem H3K27M-DMG (n=206, brown, median OS = 11.9 months). Historical controls derived from Pratt *et al.* (2018) *Acta Neuropathologica*.

(**D**) Kaplan-Meier curve (Y-axis, % overall survival; X-axis, time in months) comparing OS from diagnosis for 35 patients with non-recurrent H3K27M-DMG treated with ONC201 from both studies (n=35, orange, median OS = 21.7 months) *versus* OS in historical controls screened for early deaths (defined as OS <3 months from diagnosis, n=254, gray, median OS = 12.7 months). Historical controls derived from Pratt *et al.* (2018) *Acta Neuropathologica*.

FIGURE S6

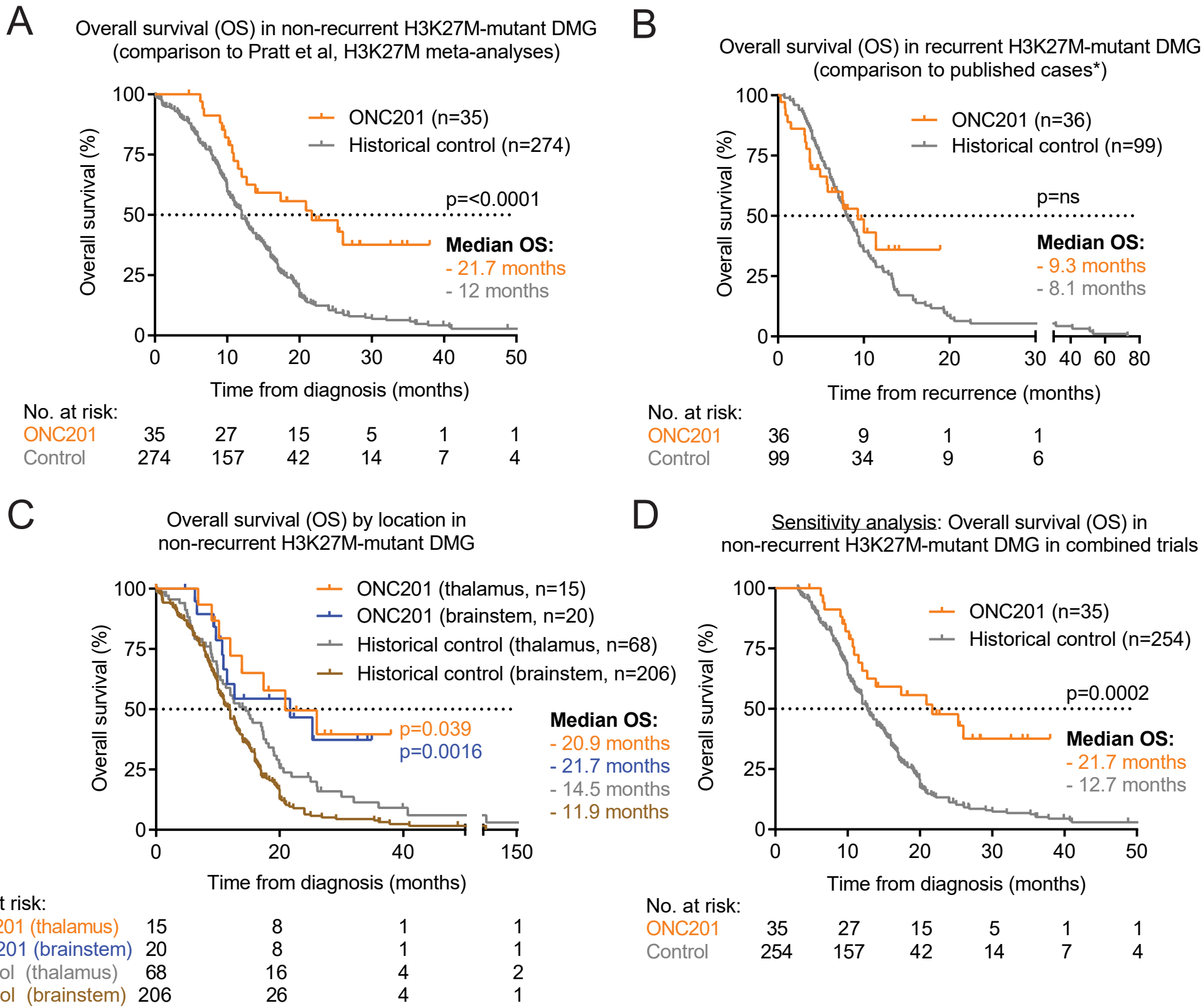
A
Overall survival (OS) in non-recurrent H3K27M-mutant DMG
(comparison to Pratt et al, H3K27M meta-analyses)
Overall survival (%)
100
75
50
25
0
ONC201 (n=35)
Historical control (n=274)
p=<0.0001
Median OS:
- 21.7 months
- 12 months
0 10 20 30 40 50
Time from diagnosis (months)
No. at risk:
ONC201 35 27 15 5 1 1
Control 274 157 42 14 7 4
B
Overall survival (OS) in recurrent H3K27M-mutant DMG
(comparison to published cases*)
Overall survival (%)
100
75
50
25
0
ONC201 (n=36)
Historical control (n=99)
p=ns
Median OS:
- 9.3 months
- 8.1 months
0 10 20 30 40 60 80
Time from recurrence (months)
No. at risk:
ONC201 36 9 1 1
Control 99 34 9 6
C
Overall survival (OS) by location in
non-recurrent H3K27M-mutant DMG
Overall survival (%)
100
75
50
25
0
ONC201 (thalamus, n=15)
ONC201 (brainstem, n=20)
Historical control (thalamus, n=68)
Historical control (brainstem, n=206)
p=0.039
p=0.0016
Median OS:
- 20.9 months
- 21.7 months
- 14.5 months
- 11.9 months
0 20 40 150
Time from diagnosis (months)
No. at risk:
ONC201 (thalamus) 15 8 1 1
ONC201 (brainstem) 20 8 1 1
Control (thalamus) 68 16 4 2
Control (brainstem) 206 26 4 1
D
Sensitivity analysis: Overall survival (OS) in
non-recurrent H3K27M-mutant DMG in combined trials
Overall survival (%)
100
75
50
25
0
ONC201 (n=35)
Historical control (n=254)
p=0.0002
Median OS:
- 21.7 months
- 12.7 months
0 10 20 30 40 50
Time from diagnosis (months)
No. at risk:
ONC201 35 27 15 5 1 1
Control 254 157 42 14 7 4

Fig. S7. Survival of patients with H3K27M-DMG treated with ONC201 versus ONC201-untreated patients (PNOC003 or HERBY Phase II trials).

(**A**) Kaplan-Meier curve (Y-axis, % overall survival; X-axis, time in months) comparing OS from diagnosis for patients with non-recurrent brainstem H3K27M-DMG treated with ONC201 (n=20, orange; median OS = 21.7 months) *versus* non-recurrent brainstem DMG from PNOC003 (n=28, gray, median OS = 11.6 months). Data for the PNOC003 trial derived from Kline *et al.* (2022) *Clin Cancer Res.*

(**B**) Kaplan-Meier curve (Y-axis, % overall survival; X-axis, time in months) comparing PFS from diagnosis for patients with non-recurrent brainstem H3K27M-DMG treated with ONC201 (n=20, orange; median PFS = 11.2 months) *versus* non-recurrent brainstem DMG from PNOC003 (n=25; gray, median PFS = 8.1 months). Data for the PNOC003 trial derived from Kline *et al.* (2022) *Clin Cancer Res*.

(**C**) Kaplan-Meier curve (Y-axis, % overall survival; X-axis, time in months) comparing OS from diagnosis for patients with non-recurrent thalamic H3K27M-DMG treated with ONC201 (n=15, orange; median OS = 26 months) *versus* non-recurrent thalamic DMG from HERBY Phase II (n=24, gray; median OS = 14.2 months). Data for the HERBY Phase II trial derived from Grill *et al.* (2018) *J Clin Oncol.*

FIGURE S7

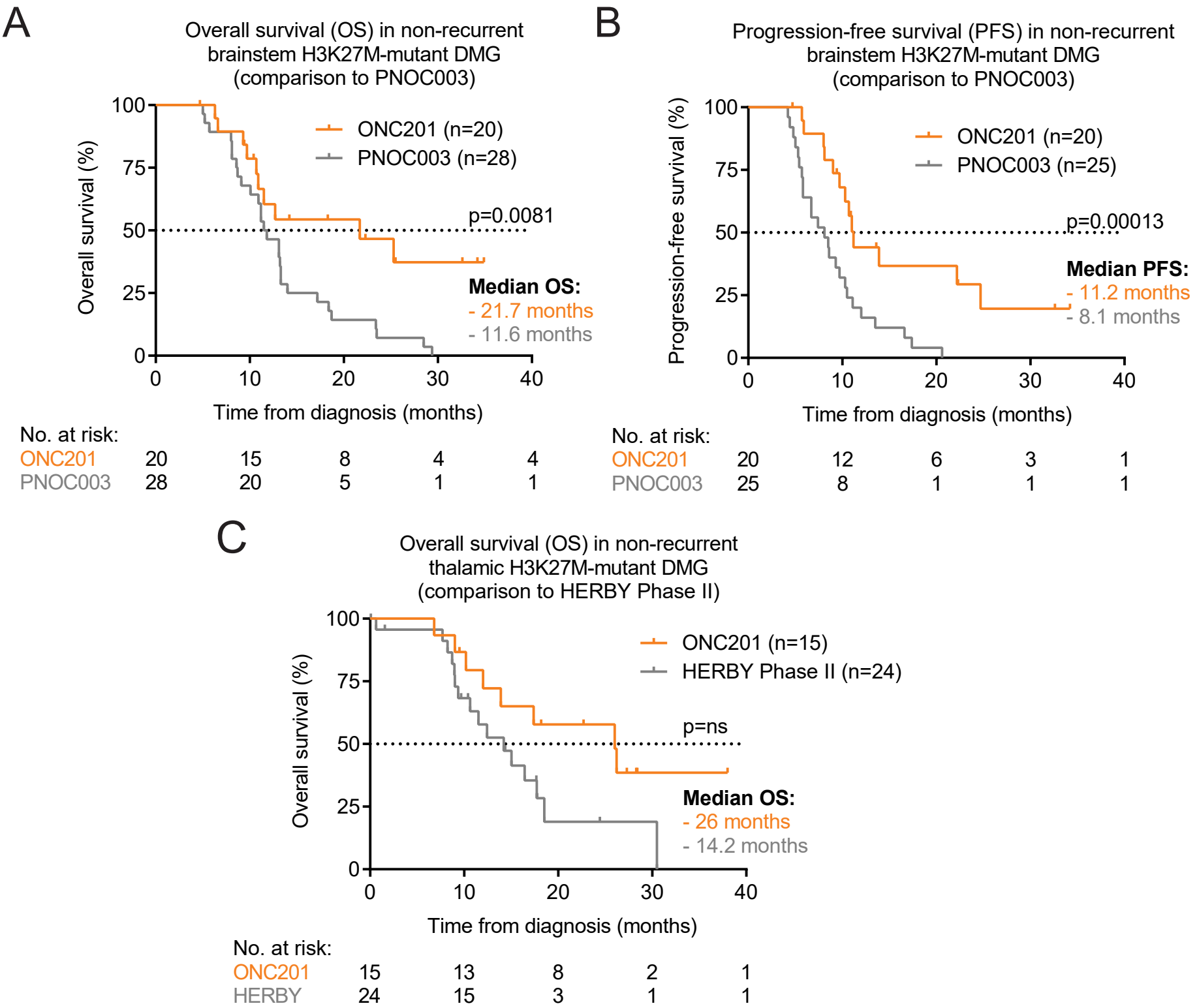
A
Overall survival (OS) in non-recurrent brainstem H3K27M-mutant DMG (comparison to PNOC003)
Overall survival (%)
100
75
50
25
0
ONC201 (n=20)
PNOC003 (n=28)
p=0.0081
Median OS:
- 21.7 months
- 11.6 months
0
10
20
30
40
Time from diagnosis (months)
No. at risk:
ONC201 20 15 8 4 4
PNOC003 28 20 5 1 1
B
Progression-free survival (PFS) in non-recurrent brainstem H3K27M-mutant DMG (comparison to PNOC003)
Progression-free survival (%)
ONC201 (n=20)
PNOC003 (n=25)
p=0.00013
Median PFS:
- 11.2 months
- 8.1 months
Time from diagnosis (months)
No. at risk:
ONC201 20 12 6 3 1
PNOC003 25 8 1 1 1
C
Overall survival (OS) in non-recurrent thalamic H3K27M-mutant DMG (comparison to HERBY Phase II)
Overall survival (%)
ONC201 (n=15)
HERBY Phase II (n=24)
p=ns
Median OS:
- 26 months
- 14.2 months
Time from diagnosis (months)
No. at risk:
ONC201 15 13 8 2 1
HERBY 24 15 3 1 1

Fig. S8. Molecular attributes of patients with H3K27M-DMG treated with ONC201.

(A) Correlation between gene expression levels (RNA) and best tumor response in non-recurrent H3K27M-mutant DMG. Best tumor response was defined as percentage radiographic reduction in tumor area relative to diagnosis. Spearman's ρ statistic (*P<0.05) was used to estimate a rank-based measure of association between gene expression and radiographic response.

(**B**) Significant TCA cycle-related genes (red) with positive correlation from **Fig. 3C** are depicted. Genes with Spearman's coefficient >5 and <5 (Y-axis) are plotted against gene rank (X-axis).

PDHB = Pyruvate Dehydrogenase B; SDHB = Succinate Dehydrogenase B; FH = Fumarate Hydratase; and ACLY = ATP Citrate Lyase.

(**C-D**) Significant (**C**) mitochondrial OXPHOS- and (**D**) steroid biosynthesis-related genes (black) with positive correlation from **Fig. 3C** are depicted. Genes with Spearman's coefficient >5 and <5 (Y-axis) are plotted against gene rank (X-axis).

NDUFB6 = NADH:Ubiquinone Oxidoreductase Subunit B6; COX16 = Cytochrome C Oxidase Assembly Factor 16; ATP1A1 = ATPase Na+/K+ Transporting Subunit Alpha 1; NDUFAB1 = NADH:Ubiquinone Oxidoreductase Subunit AB1; COX11 = Cytochrome C Oxidase Assembly Factor 11; ATP6V0A1 = ATPase H+ Transporting V0 Subunit A1; PPA1 = Inorganic Pyrophosphatase 1; and NDUFA6 = NADH:Ubiquinone Oxidoreductase Subunit A6.

SQLE = Squalene Epoxidase; DHCR7 = 7-Dehydrocholesterol Reductase; LIPA = Lipase A, Lysosomal Acid Type; MSMO1 = Methylsterol Monooxygenase 1; SC5D = Sterol-C5-Desaturase; and HSD17B7 = Hydroxysteroid 17-Beta Dehydrogenase 7.

(**E**) Significant T cell receptor signaling pathway-related genes (black) with negative correlation from **Fig. 3C** are depicted. Genes with Spearman's coefficient >5 and <5 (Y-axis) are plotted against gene rank (X-axis).

CD247; CD28; ZAP70 = Zeta Chain of T Cell Receptor Associated Protein Kinase 70; MAP2K7 = Mitogen-Activated Protein Kinase Kinase 7; ITK = IL2 Inducible T Cell Kinase; NFATC1 = Nuclear Factor Of Activated T Cells 1; and IKBKB = Inhibitor Of Nuclear Factor Kappa B Kinase Subunit Beta.

FIGURE S8

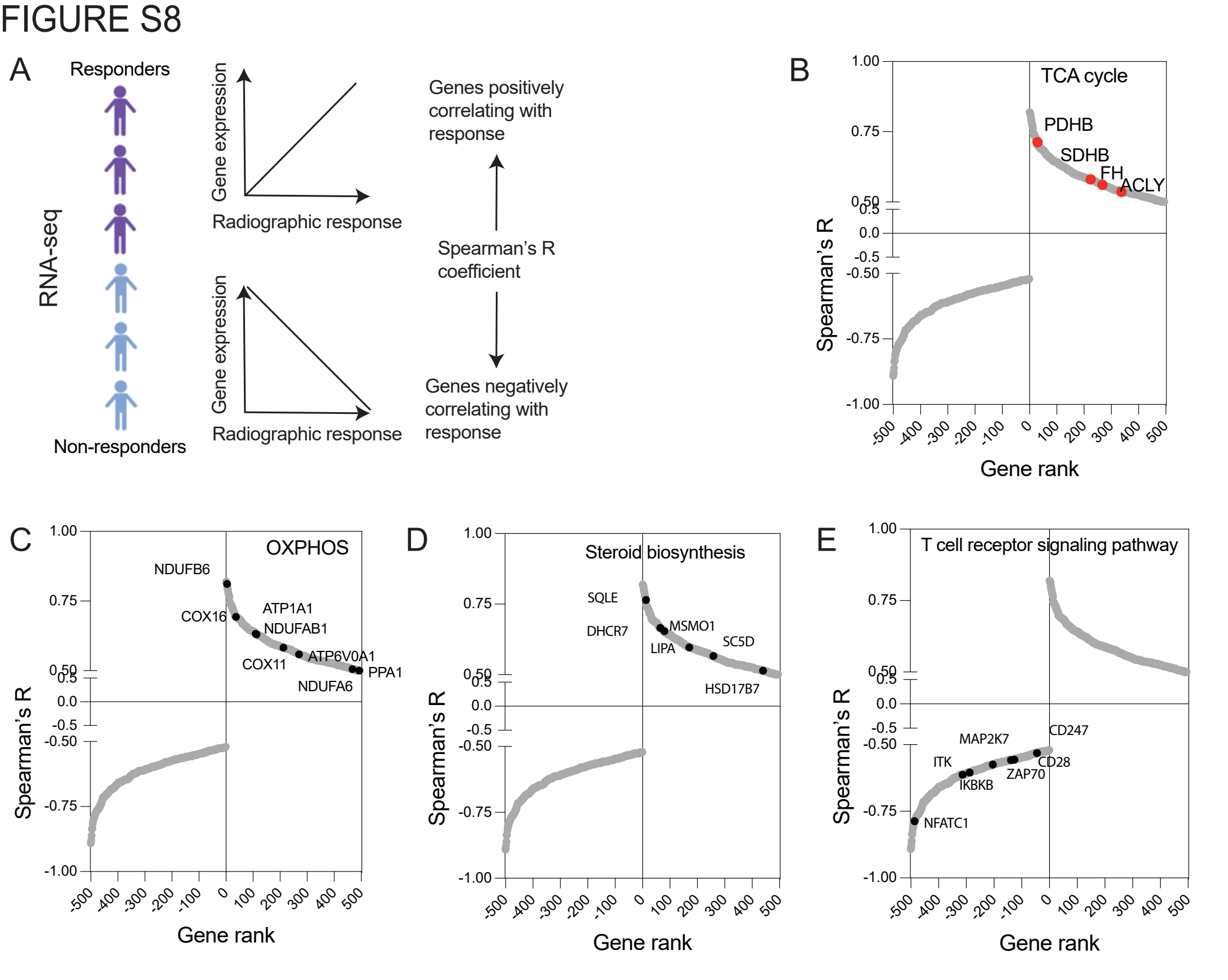
A
Responders
RNA-seq
Non-responders
Gene expression
Radiographic response
Gene expression
Radiographic response
Genes positively correlating with response
Spearman's R coefficient
Genes negatively correlating with response
B
TCA cycle
PDHB
SDHB
FH
ACLY
Spearman's R
Gene rank
C
OXPHOS
NDUFB6
COX16
ATP1A1
NDUFAB1
COX11
ATP6V0A1
PPA1
NDUFA6
Spearman's R
Gene rank
D
Steroid biosynthesis
SQLE
DHCR7
MSMO1
LIPA
SC5D
HSD17B7
Spearman's R
Gene rank
E
T cell receptor signaling pathway
MAP2K7
CD247
ITK
CD28
ZAP70
IKBKB
NFATC1
Spearman's R
Gene rank

Fig. S9: Survival of H3K27M-DMG mice models treated with ONC201.

(**A**) Cartoon depicting procedure for generating immune-competent *in utero* electroporation mouse models of H3K27M-DMG. "PPK" mice harbor dominant-negative TP53, PDGFRA D842V, and H3F3A (H3.3) K27M mutations.

(**B**) Kaplan-Meier curves comparing OS from days post-birth in ONC201-treated (orange, n=6*) versus* vehicle (black, n=7) PPK mice models. Mice were treated with 125 mg/kg ONC201 once a week.

(**C**) Kaplan-Meier curves comparing OS from days post-implantation in ONC201-treated (orange, n=10) *versus* vehicle (black, n=9) patient-derived xenograft mice models. Mice were treated with 100 mg/kg ONC201 once a week.

FIGURE S9

A

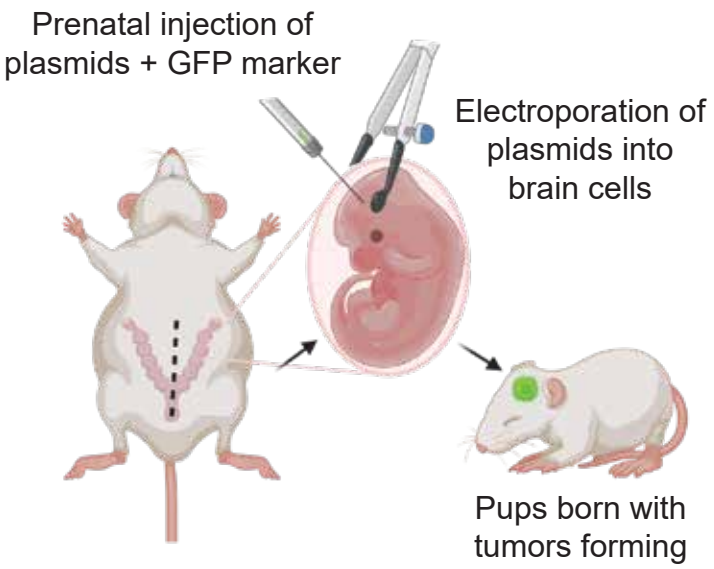

B

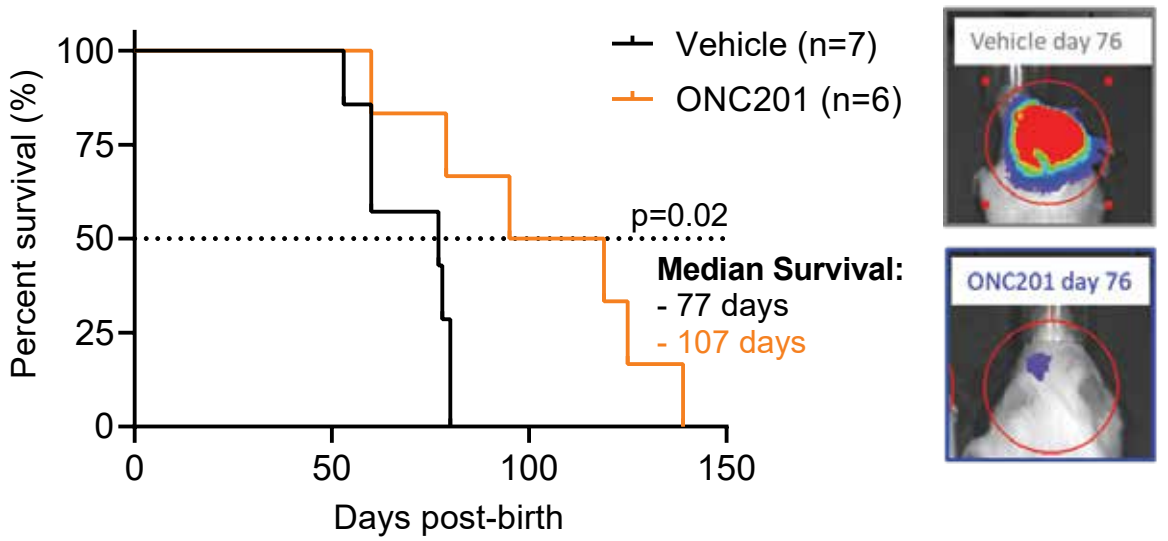

C

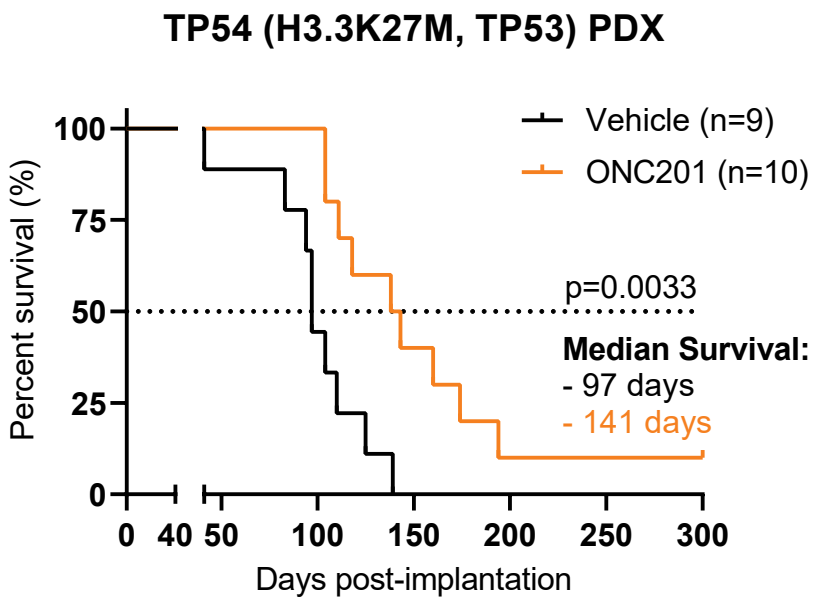

Fig. S10. Integrative analysis of *in vitro* and human tumor metabolic gene expression in response to ONC201.

(**A**) Mouse pharmacokinetic study to assess brain penetration and tissue concentrations of ONC201. Schema (left) showing mice (n=3) injected intraperitoneally (IP) with 15 mg/kg of ONC201. After 30 minutes, plasma and tissues from midline locations harboring H3K27M-DMGs (spinal cord = blue, brainstem = teal, thalamus = green) were harvested. Bar graph (right) showing ONC201 concentrations (Y-axis, μM) assessed by LC/MS quantification from plasma and three midline brain locations (n=3 per location).

(**B**) Dose response curves (Y-axis, cell viability normalized to vehicle treatment) for four low passage H3.3K27M-DMG, patient-derived cell lines (DIPG007, QCTB-R095, DIPGXIII*P, and SF7761; n=3 for each cell line) at indicated concentrations of ONC201 (X-axis, μM) for 72 hours. Values (right) for half maximal inhibitory concentration (IC_{50}) and ONC201 efficacy (maximal effect, E_{max}) are indicated.

(**C**) Seahorse time course data of glycolysis stress test showing extracellular acidification rate (ECAR, mPH/min/10,000 cells, Y-axis) plotted against time (minutes, X-axis) in H3.3K27M-DMG cells DIPG007, QCTB-R095, and DIPGXIII*P. Each cell line (n=6-8) was untreated (black) or treated with vehicle (blue), 5 μM ONC201 (red), or 10 μM ONC201 (orange).

(**D**) Seahorse time course data of oxidative phosphorylation stress test showing oxygen consumption rate (OCAR, pMols/min/10,000 cells, Y-axis) plotted against time (minutes, X-axis) in H3.3K27M-DMG cells DIPG007, QCTB-R095, and DIPGXIII*P. Each cell line (n=6-8) was untreated (black) or treated with vehicle (blue), 5 μM ONC201 (red), or 10 μM ONC201 (orange).

(**E**) Pathway impact analysis plot of upregulated genes and metabolites from **Fig. 4A** and **Fig. 4B** (X-axis, pathway impact, ONC201 *versus* vehicle; Y-axis, corresponding -Log10 *P*).

(**F**) Immunoblots for Hexokinase 2 (HK2) in H3.3K27M DIPG-XIII*P, DIPG007, and SF7761 treated with or without indicated concentrations of ONC201 for 48 hours. Vinculin was probed as loading control.

(**G**) Schema (left) of [$^{13}C_6$]-glucose tracing into the TCA cycle indicating predicted mass isotopes (M+3 or M+2) for each metabolite. Bar graph (right) showing fraction enrichment (Y-axis) for M+3 pyruvate (Pyr), M+3 lactate (Lac), M+2 α-ketoglutarate (α-KG), M+2 fumarate (Fum), M+2 malate (Mal), and M+2 aspartate (Asp) are indicated in cells treated with vehicle (blue) or 5 μM ONC201 (red). n=3 replicates per condition.

FIGURE S10

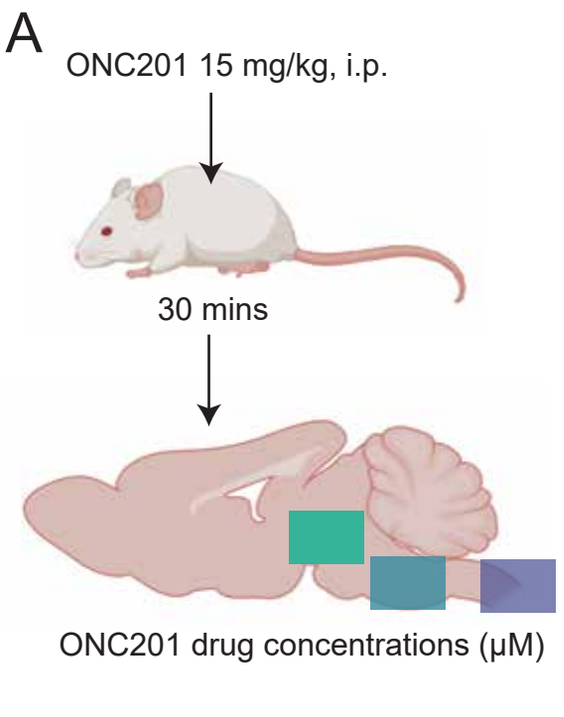

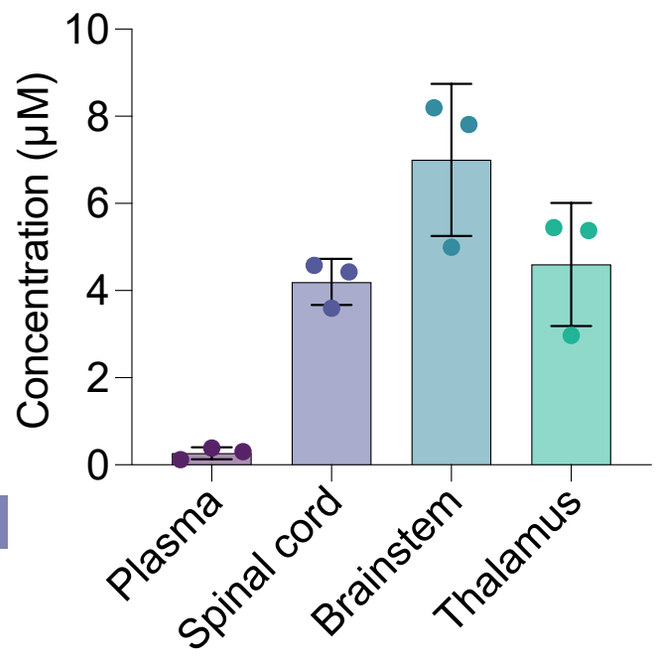

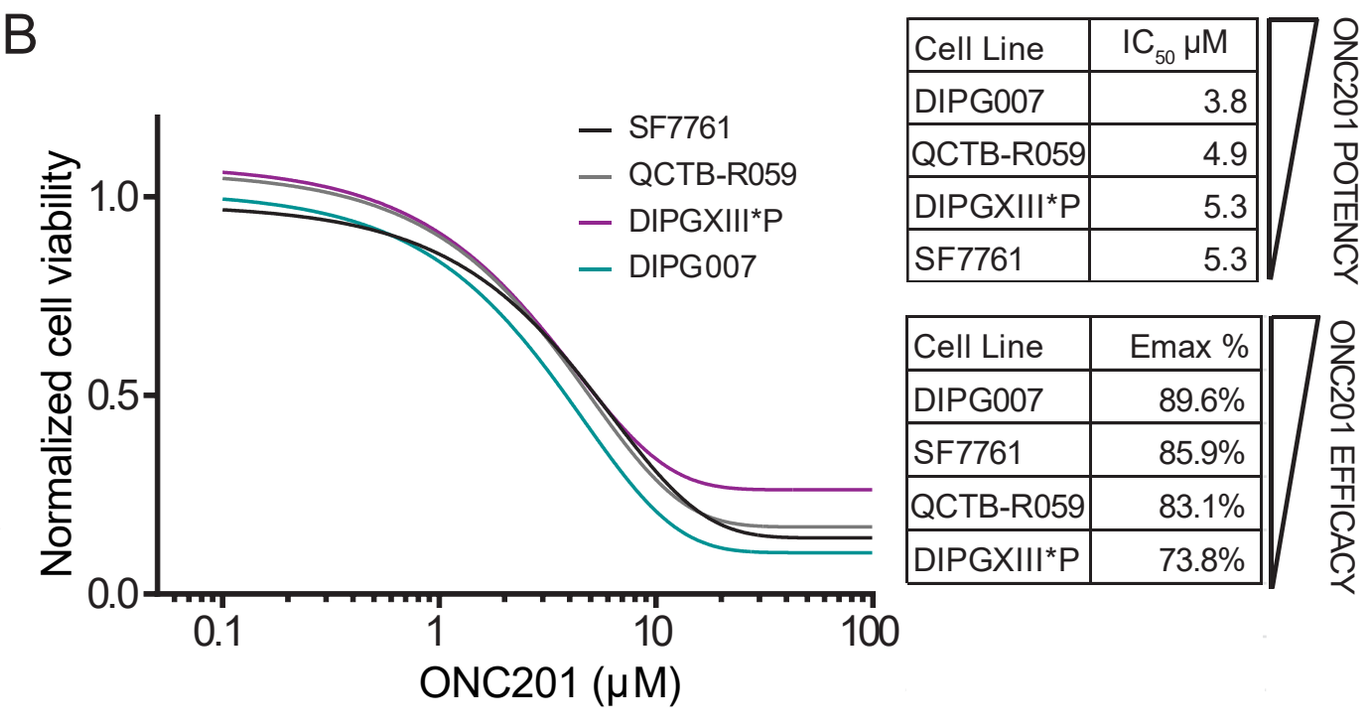

Cell Line	IC_{50} μM
DIPG007	3.8
QCTB-R059	4.9
DIPGXIII*P	5.3
SF7761	5.3

ONC201 POTENCY

Cell Line	Emax %
DIPG007	89.6%
SF7761	85.9%
QCTB-R059	83.1%
DIPGXIII*P	73.8%

ONC201 EFFICACY

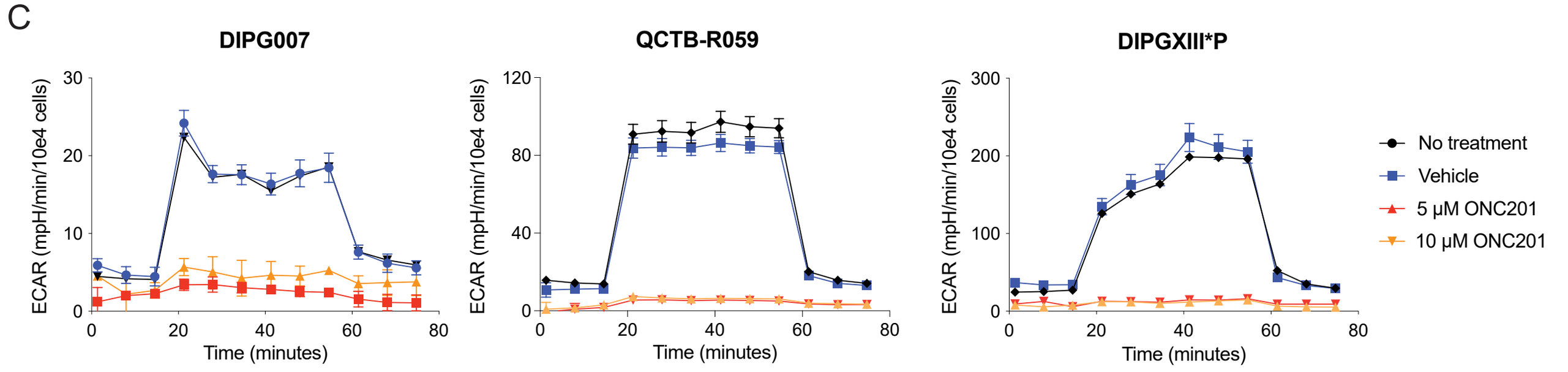

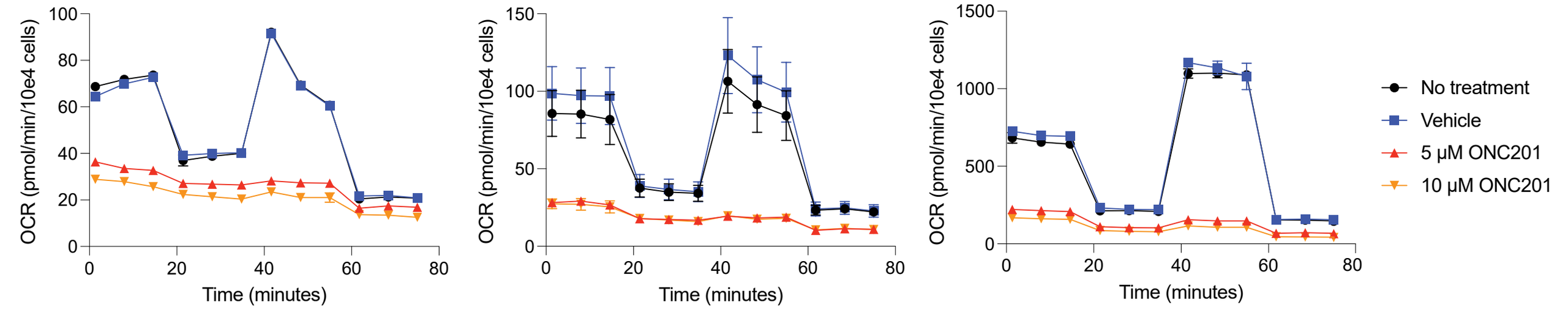

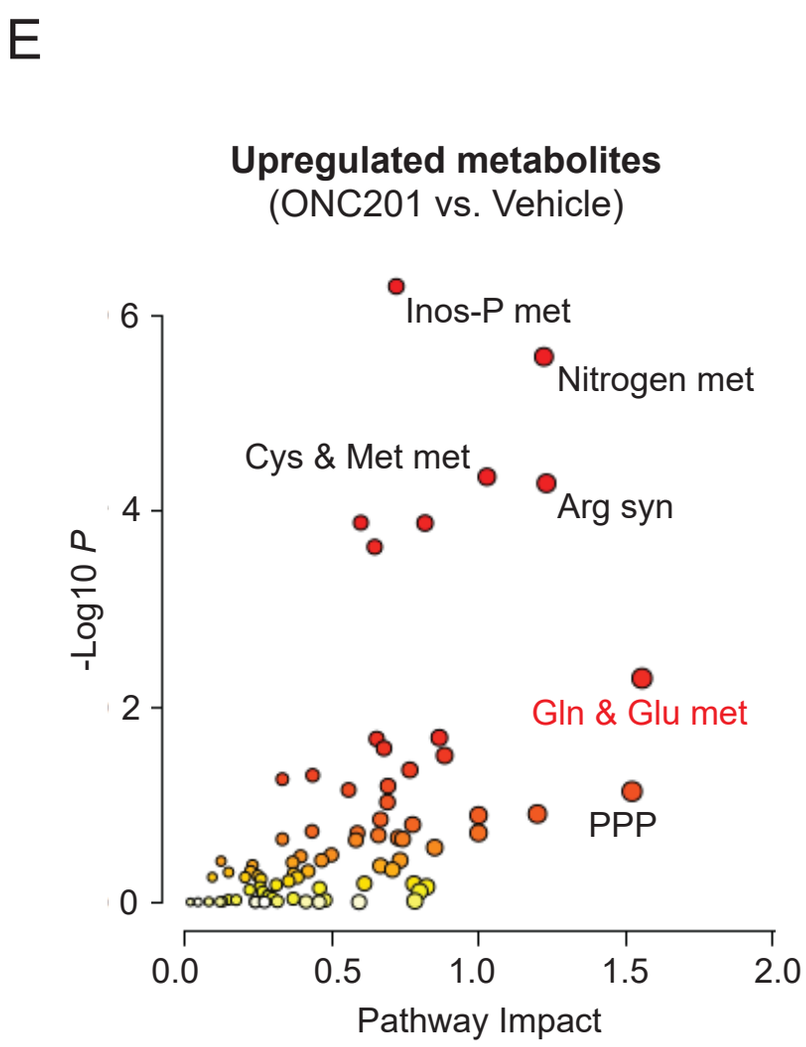

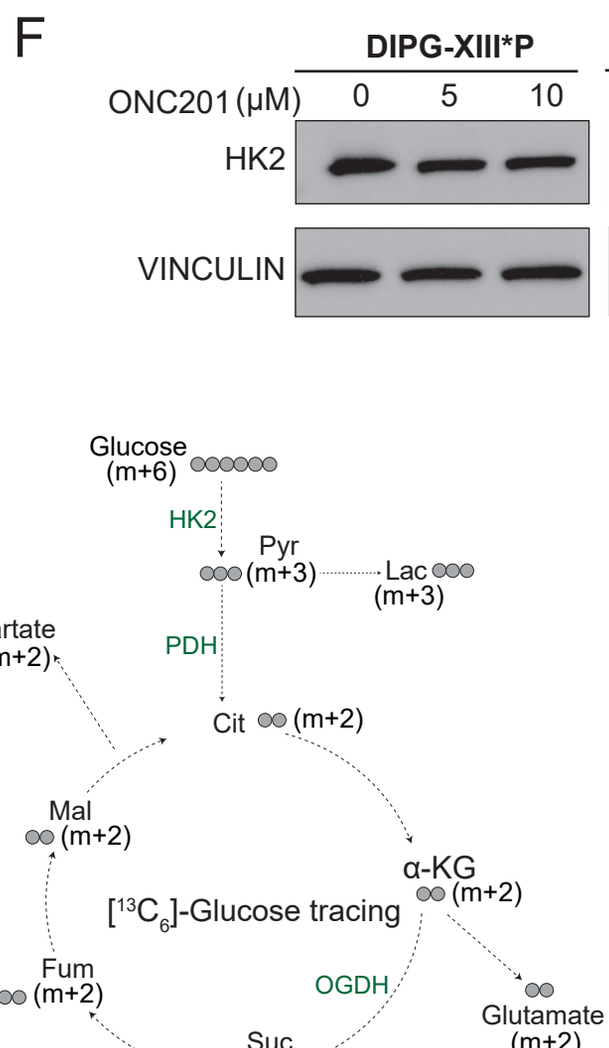

Fig. S11. ONC201-mediated L2HG production increases H3K27me3 in H3K27M-DMG cells.

(**A**) Representative traces from enantiomer-specific mass spectroscopy for L-2HG from DIPG-XIII*P cells treated with vehicle (blue) or ONC201 (red, 5 μM, 48 hours); note earlier retention time between 27-29 minutes.

(**B**) Representative trace from enantiomer-specific mass spectroscopy for D-2HG in IDH1 R132H-mutant TB096 patient-derived cell line; note later retention time between 32-35 minutes.

(**C**) H3.3K27M (DIPG007 and DIPGXIII*P) and H3.1K27M (DIPGIV) cells were treated with indicated concentrations of ONC201 for 48 hours. Cells were probed for H3K27me3 and total H3 (as loading control). Arrowhead indicates increased H3K27me3 across all cell lines.

(**D**). H3.3K27M and H3WT expressing isogenic mouse neuronal stem cells (mNSC) were treated with ONC201 (5 or 10 μM) for 48 hours. Cells were probed for H3K27me3 and total H3 (as loading control). Arrowhead indicates increased H3K27me3.

(**E-F**). Image-J based quantification of H3K27me3/total H3 ratios (Y-axis) from H3.3K27M mNSC (**E**) and H3WT mNSC (**F**) in **Supplementary Fig. S11D**.

(**G**) Immunoblots for H3K27me3 and total H3 (as loading control) in H3.3K27M DIPG007 and SF7761 cell lines treated with indicated concentrations of L-2HG or vehicle.

(**H**) Immunoblots for H3K27ac and total H3 (as loading control) in H3.3K27M DIPG007, SF7761, and mNSC cell lines treated with indicated concentrations of ONC201 or vehicle.

(**I**) Immunoblots for HIF-1α in 293T and H3.3K27M DIPG007 and DIPGXIII*P cell lines. Cells were treated with 200 μM of HIF-1α stabilizer deferoxamine as positive control or with indicated concentrations of ONC201. β-actin was probed as loading control.

FIGURE S11

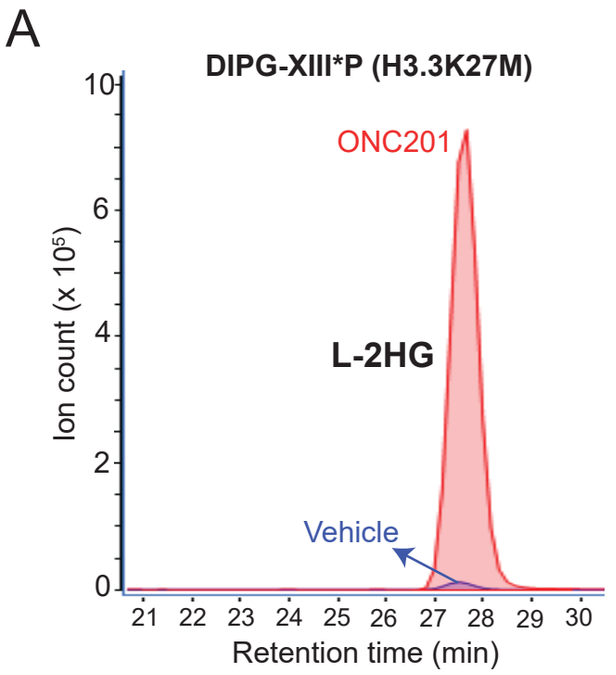
A
DIPG-XIII*P (H3.3K27M)
ONC201
L-2HG
Vehicle
Ion count (x 10^5)
Retention time (min)

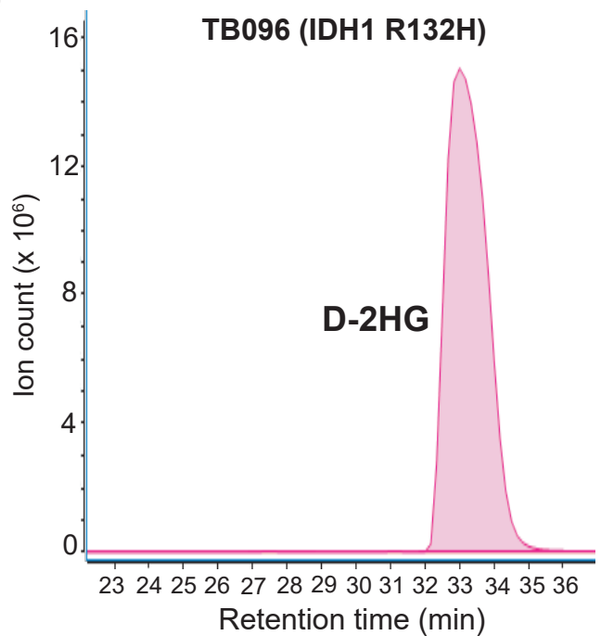
B
TB096 (IDH1 R132H)
D-2HG
Ion count (x 10^6)
Retention time (min)

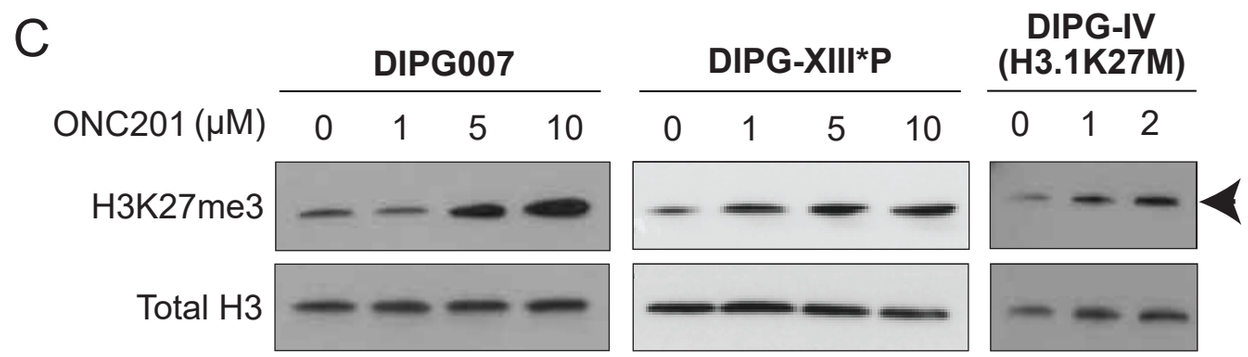
C
DIPG007
DIPG-XIII*P
DIPG-IV (H3.1K27M)
ONC201 (μM)
H3K27me3
Total H3

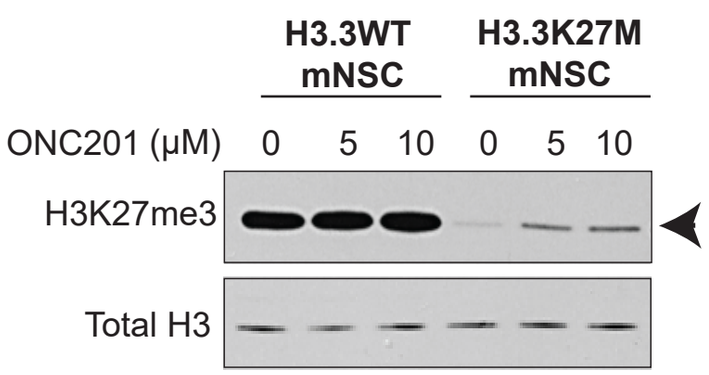
D
H3.3WT mNSC
H3.3K27M mNSC
ONC201 (μM)
H3K27me3
Total H3

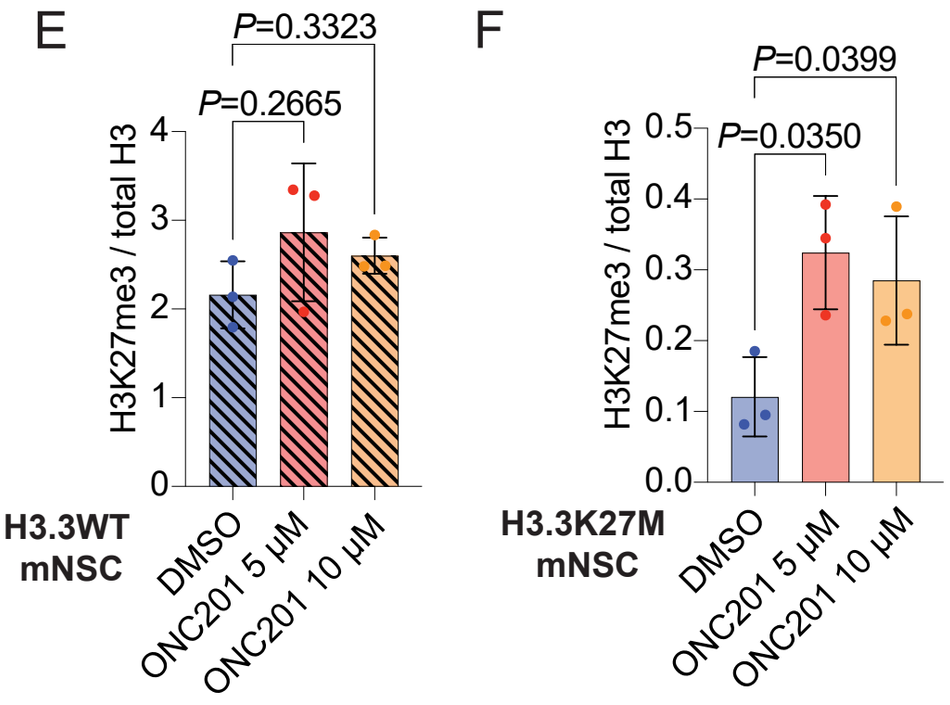
E
P=0.3323
P=0.2665
H3K27me3 / total H3
H3.3WT mNSC
DMSO
ONC201 5 μM
ONC201 10 μM

F
P=0.0399
P=0.0350
H3K27me3 / total H3
H3.3K27M mNSC
DMSO
ONC201 5 μM
ONC201 10 μM

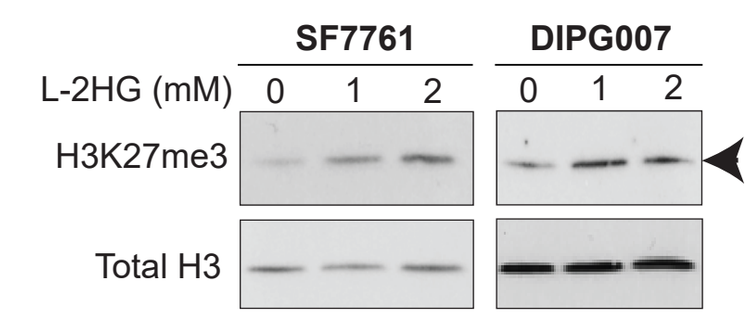
G
SF7761
DIPG007
L-2HG (mM)
H3K27me3
Total H3

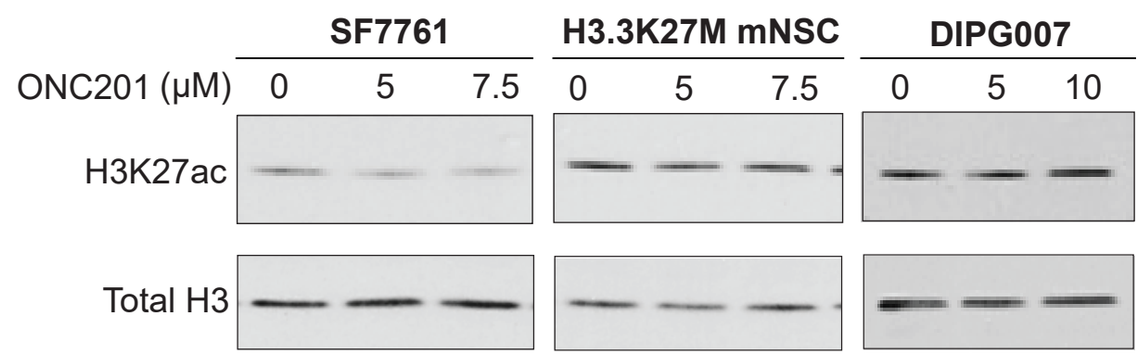
H
SF7761
H3.3K27M mNSC
DIPG007
ONC201 (μM)
H3K27ac
Total H3

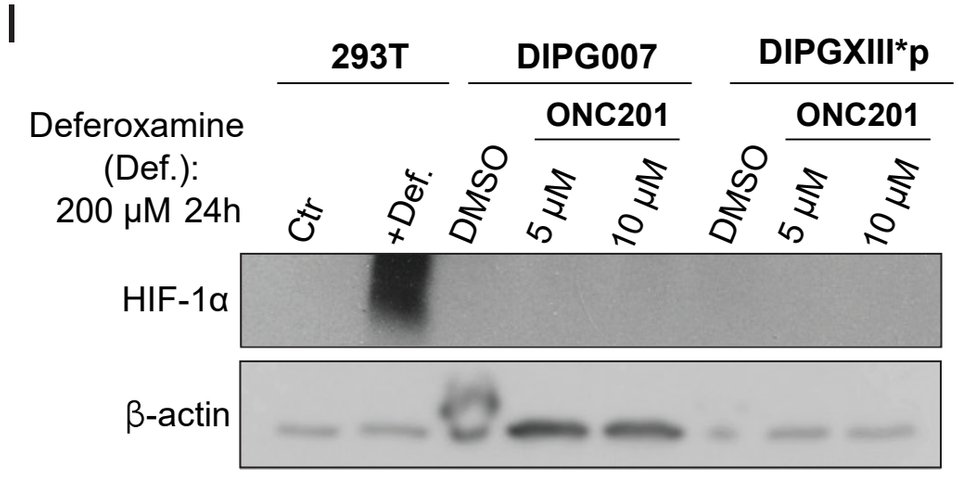
I
293T
DIPG007
DIPGXIII*p
ONC201
Deferoxamine (Def.): 200 μM 24h
Ctr
+Def.
DMSO
5 μM
10 μM
HIF-1α
β-actin

Fig. S12. ONC201-induced increase in H3K27me3 is mediated by lactate dehydrogenase.

(**A**) Immunoblot for LDHA in DIPG007 cells transduced with two independent shRNAs against LDHA. Vinculin was used as loading control.

(**B**) Immunoblots for H3K27me3 and total H3 (as loading control) in DIPG007 cells with or without LDHA knockdown or treated with LDH pharmacologic inhibitors GSK-2837808A or oxamate in the presence and absence of ONC201 (5 μM, 48 hours). Arrowhead indicates no change in H3K27me3.

(**C**) (Left) Immunoblot for L-2HGDH in DIPG007 cells with or without L-2HGDH overexpression. Vinculin was used as loading control. (Right) Cells with L-2HGDH overexpression were treated with ONC201 (5 μM, 48 hours) or vehicle and probed for H3K27me3 and total H3 (as loading control). Arrowhead indicates no change in H3K27me3.

(**D**) (Left) Immunoblot for D-2HGDH in DIPG007 cells with or without D-2HGDH overexpression. Vinculin was used as loading control. (Right) Cells with D-2HGDH overexpression were treated with ONC201 (5μM, 48 hours) or vehicle and probed for H3K27me3 and total H3 (as loading control). Arrowhead indicates increase in H3K27me3.

(**E**) Immunoblots for OGDH in DIPG007 cells transduced with two independent shRNAs against OGDH. HSP90 was used as loading control. Cells were probed for H3K27me3, H3K36me3, H3K9me3, H3K4me3, H3K27M and total H3 (as loading control). Arrowhead indicates increases in H3K27me3 and H3K36me3.

(**F**) ClpP was knocked down (KD) in DIPG007 cells. Cells with or without ClpP knockdown were treated with indicated concentrations of ONC201 for 48 hours and then probed for ClpX, NDUFA12, cleaved PARP, and OGDH. α-tubulin was used as loading control.

(**G**) Normalized cell counts (Y-axis) were plotted against increasing concentrations of ONC201 (X-axis) in DIPG007 cells with ClpP KD (green) or expressing empty vector control (blue).

(**H**) Immunoblots for H3K27me3 and total H3 (as loading control) in DIPG007 cells with ClpP KD treated with 5 or 10 μM ONC201 for 48 hours. Arrowhead indicates no change in H3K27me3.

FIGURE S12

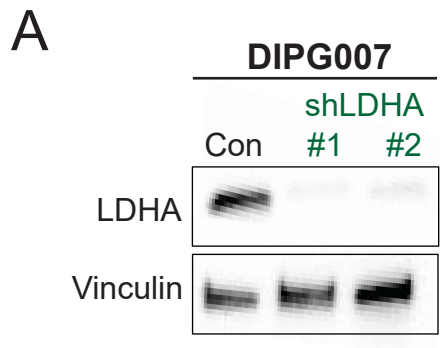
A
DIPG007
shLDHA
Con
#1
#2
LDHA
Vinculin

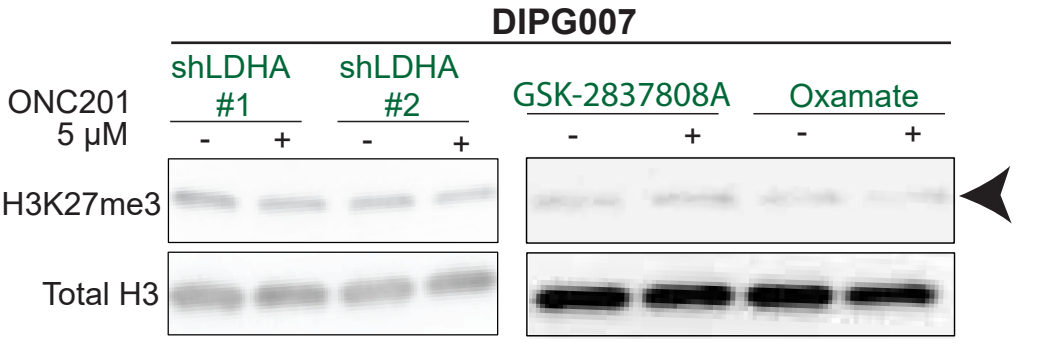
B
DIPG007
shLDHA #1
shLDHA #2
GSK-2837808A
Oxamate
ONC201 5 μM
- + - + - + - +
H3K27me3
Total H3

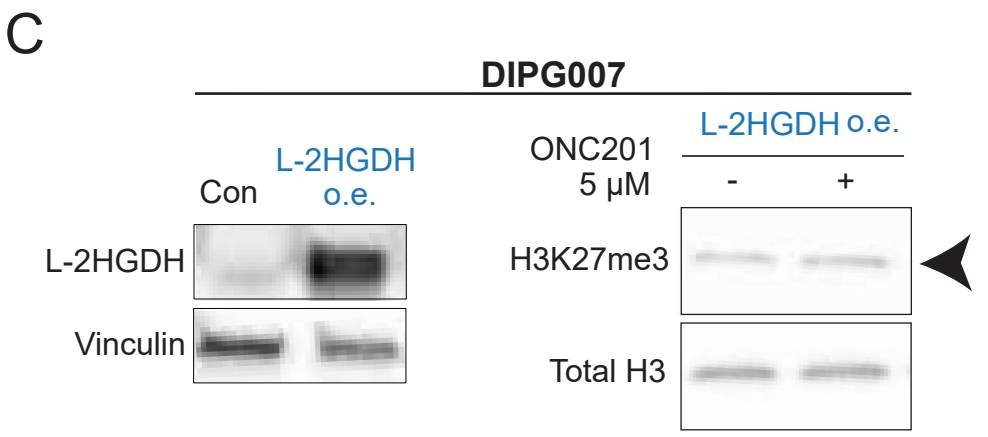
C
DIPG007
Con
L-2HGDH o.e.
L-2HGDH
Vinculin
ONC201 5 μM
L-2HGDH o.e.
- +
H3K27me3
Total H3

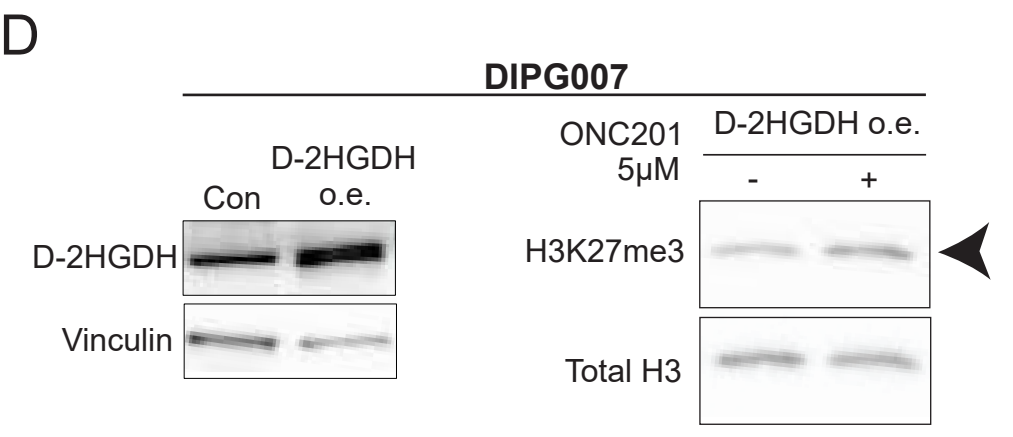
D
DIPG007
Con
D-2HGDH o.e.
D-2HGDH
Vinculin
ONC201 5μM
D-2HGDH o.e.
- +
H3K27me3
Total H3

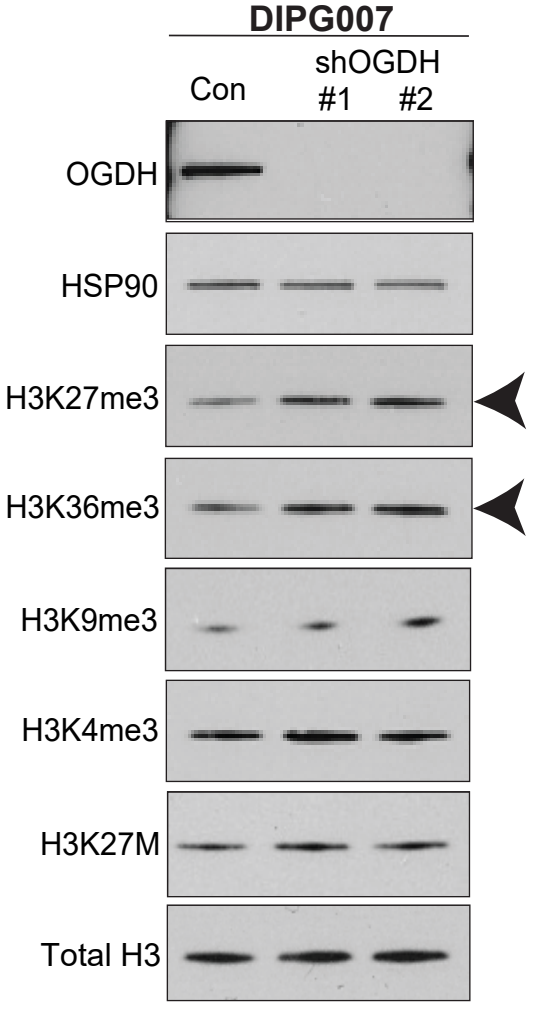
E
DIPG007
Con
shOGDH #1
shOGDH #2
OGDH
HSP90
H3K27me3
H3K36me3
H3K9me3
H3K4me3
H3K27M
Total H3

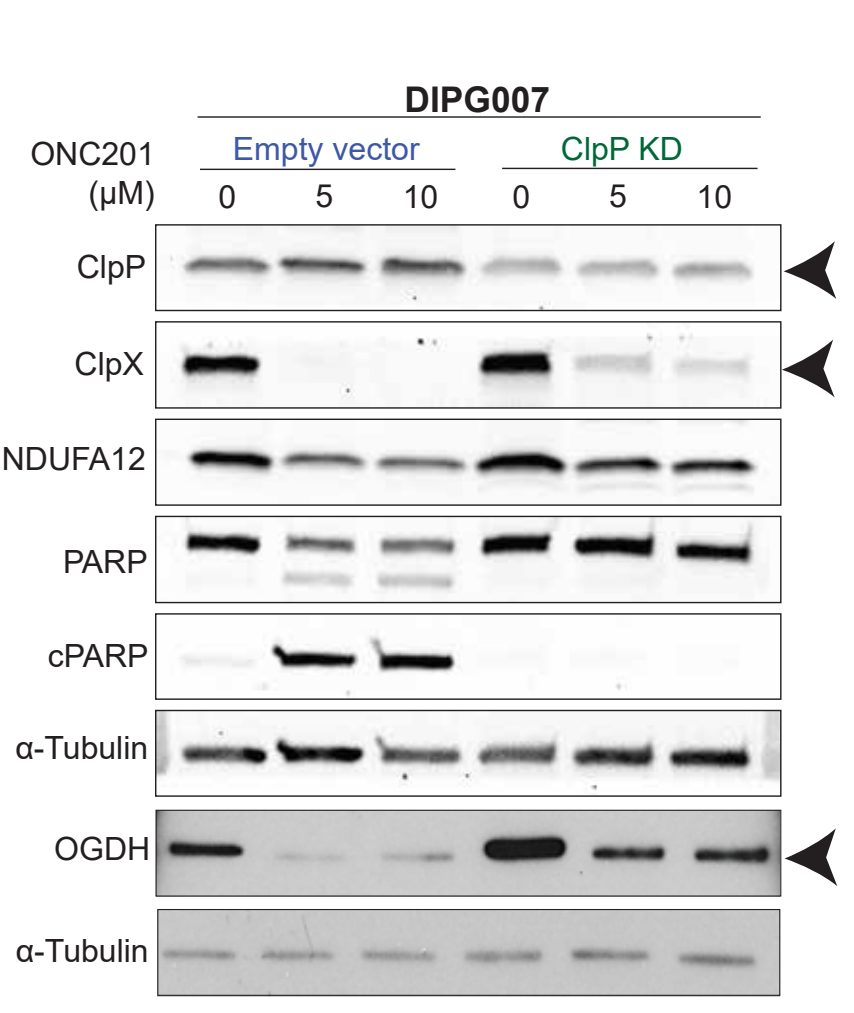
F
DIPG007
ONC201 (μM)
Empty vector
ClpP KD
0 5 10 0 5 10
ClpP
ClpX
NDUFA12
PARP
cPARP
α-Tubulin
OGDH
α-Tubulin

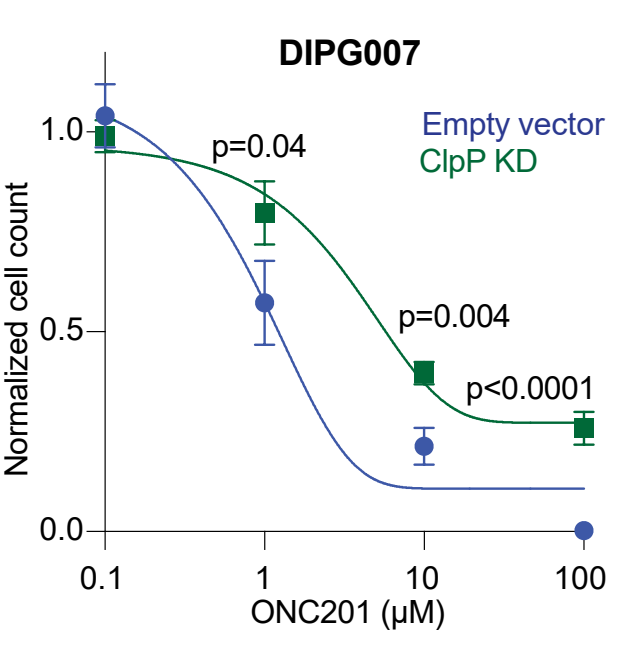
G
DIPG007
Empty vector
ClpP KD
p=0.04
p=0.004
p<0.0001
Normalized cell count
1.0
0.5
0.0
0.1
1
10
100
ONC201 (μM)

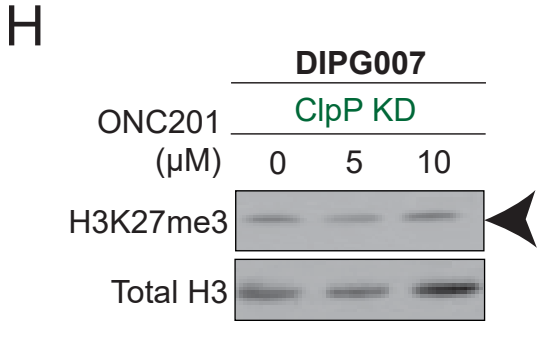
H
DIPG007
ONC201 (μM)
ClpP KD
0 5 10
H3K27me3
Total H3

Fig. S13. ONC201 alters genomic chromatin accessibility and H3K27ac distribution in H3K27M-DMG cells.

(**A**) Venn diagram depicting overlap of genes with decreased chromatin accessibility (ATAC-seq) and downregulated gene expression by RNA-seq in DIPG007 cells treated with ONC201 (5 µM, 48 hours) *versus* vehicle.

(**B**) Venn diagram depicting overlap of genes with decreased H3K27ac enrichment at promoters and enhancers and downregulated gene expression by RNA-seq in DIPG007 cells treated with ONC201 (5 µM, 48 hours) *versus* vehicle.

(**C**) Venn diagram depicting overlap of genes with decreased chromatin accessibility (ATAC-seq), decreased H3K27ac enrichment at promoters and enhancers, and downregulated gene expression by RNA-seq in DIPG007 cells treated with ONC201 (5 µM, 48 hours) *versus* vehicle.

(**D**) GSEA pathway analysis of 348 downregulated genes from Venn diagram in **Supplementary Fig. S13C** relating to cell cycle regulation and differentiation-related pathways (purple).

(**E**) Transcription factor motif analysis of downregulated H3K27ac and ATAC-seq genes showing enrichment of early lineage neuro-developmental transcription factors including *SOX10, SOX21*, and *SOX3*.

(**F**) Heatmaps showing chromatin accessibility (ATAC-seq) at promoters and enhancers (+/- 2Kb from peak center) in DIPG007 cells treated with vehicle or ONC201 (5 µM ONC201 for 48 hours; n=2 replicates per condition).

(**G**) Heatmaps showing genomic H3K27ac at promoters and enhancers (+/- 2Kb from peak center) in DIPG007 cells treated with vehicle or ONC201 (5µM ONC201 for 48 hours, n=2 replicates per condition).

(**H**) Venn diagram depicting overlap of genes with increased chromatin accessibility (ATAC-seq) and upregulated gene expression by RNA-seq in DIPG007 cells treated with ONC201 (5 µM, 48 hours) *versus* vehicle.

(**I**) GSEA pathway analysis of 1096 upregulated genes from Venn diagram in **Supplementary Fig. S13H**.

(**J**) Venn diagram depicting overlap of genes with increased H3K27ac enrichment at promoters and enhancers and upregulated gene expression by RNA-seq in DIPG007 cells treated with ONC201 (5 µM, 48 hours) *versus* vehicle.

(**K**) GSEA pathway analysis of 818 upregulated genes from Venn diagram in **Supplementary Fig. S13J**.

(**L**) Venn diagram depicting overlap of genes with increased chromatin accessibility (ATAC-seq), increased H3K27ac enrichment at promoters and enhancers, and upregulated gene expression by RNA-seq in DIPG007 cells treated with ONC201 (5 μM, 48 hours) *versus* vehicle.

(**M**) GSEA pathway analysis of 223 upregulated genes from Venn diagram in **Supplementary Fig. S13L**.

FIGURE S13

A

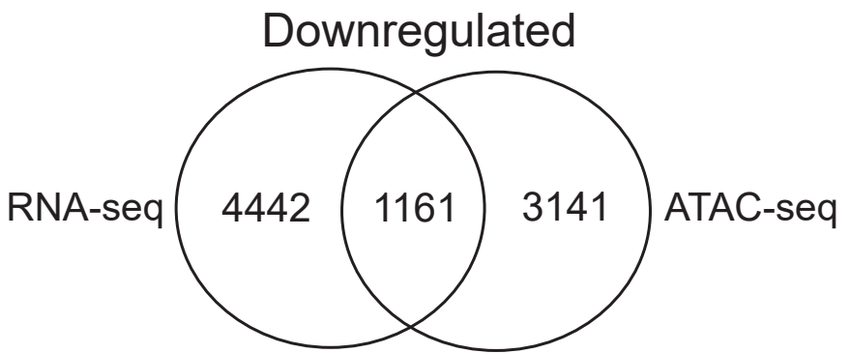

B

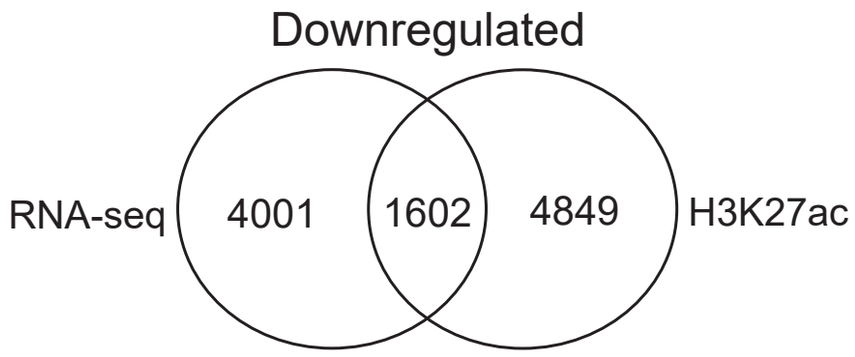

C

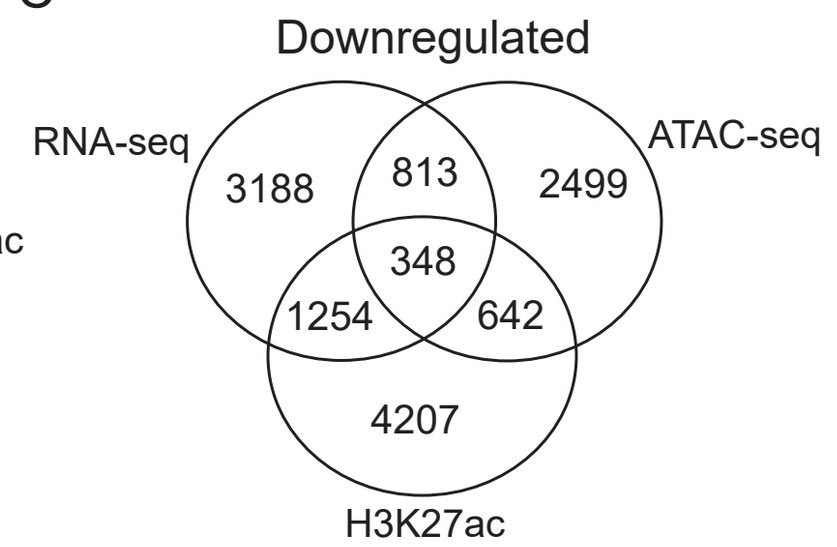

D

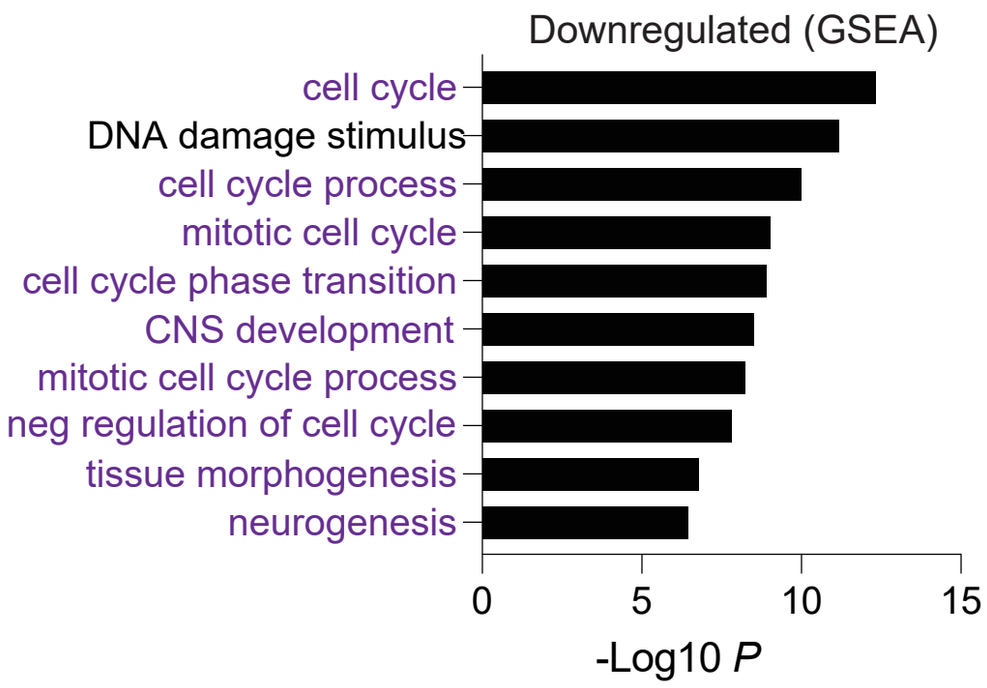

E

F

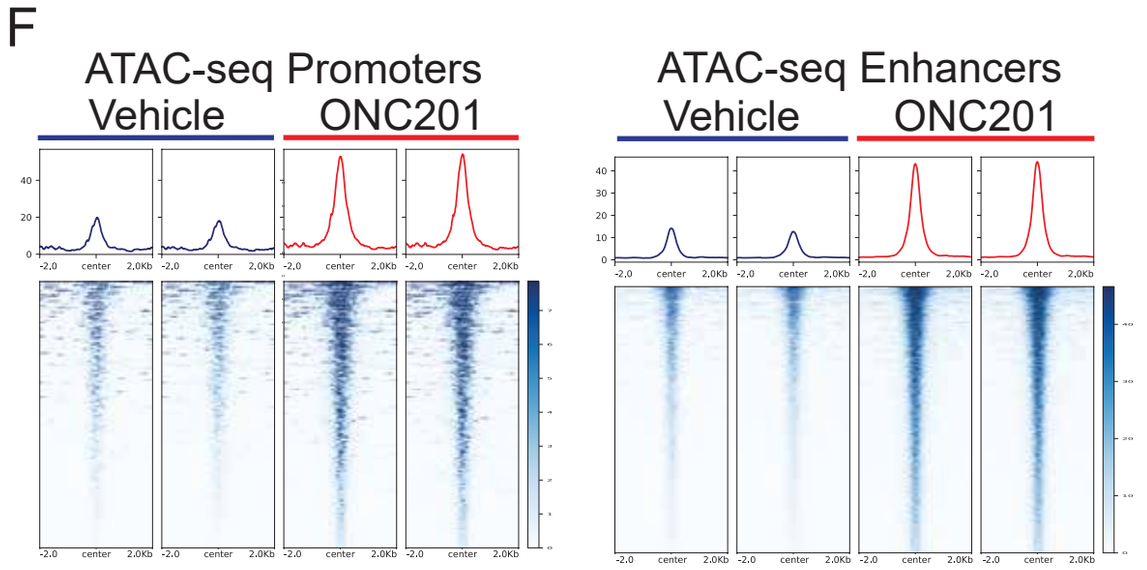

G

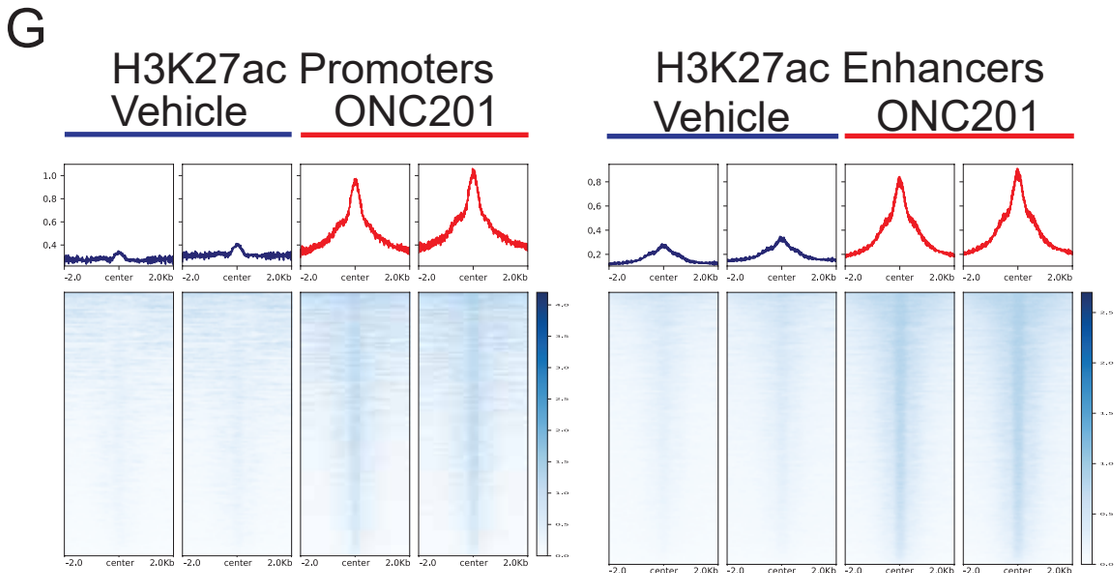

H

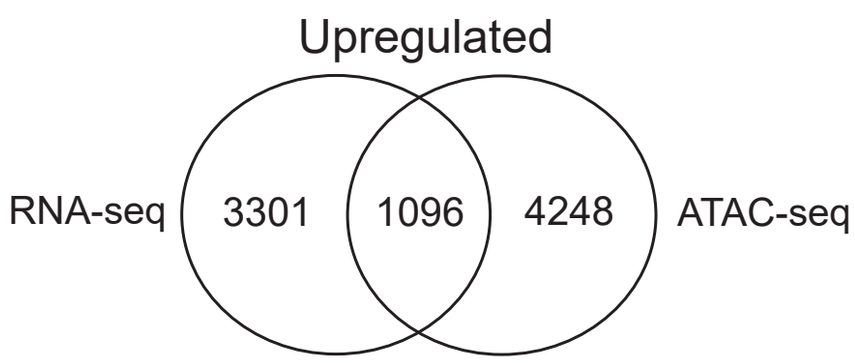

I

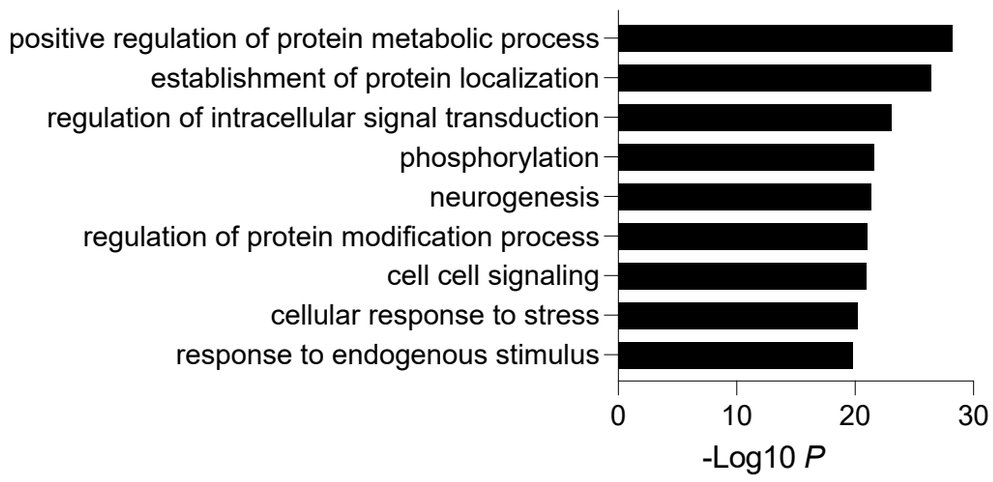

J

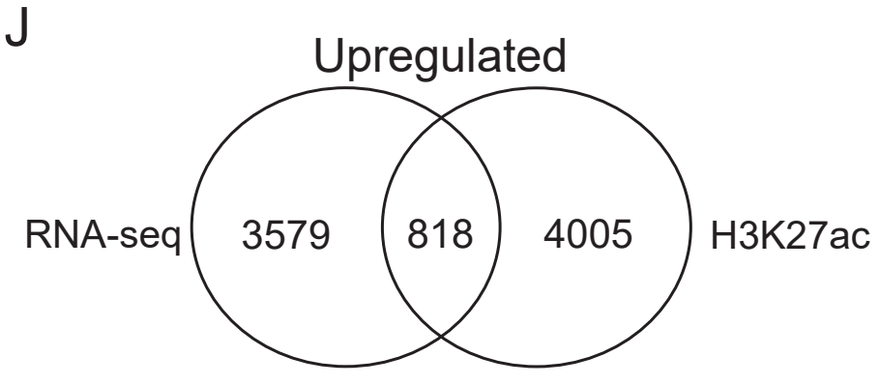

K

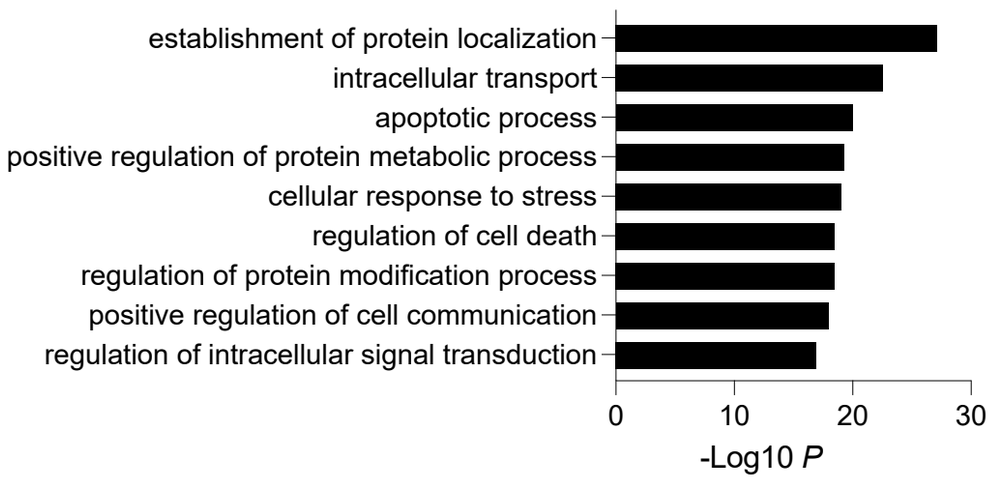

L

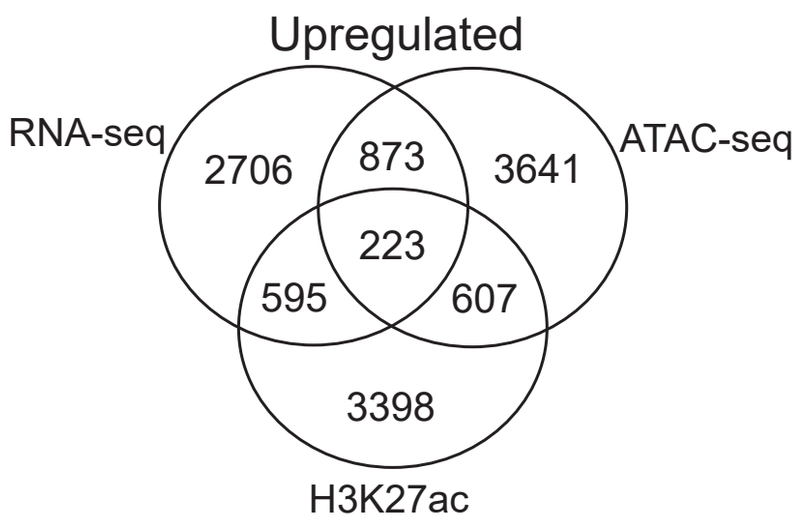

M

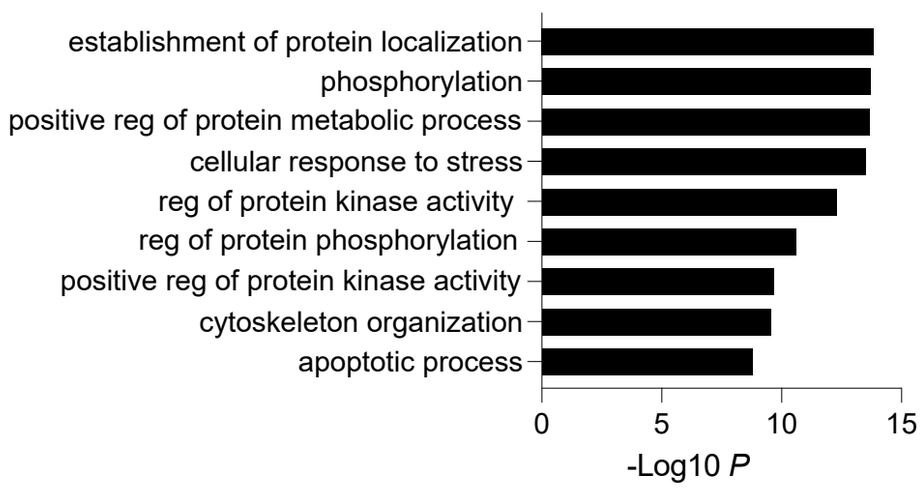

Fig. S14. ONC201 increases global H3K27me3 in patient samples.

(**A**) Representative H3K27me3 IHC images from H3K27M-DMG patients who were treated (n=6) or untreated (n=4) with ONC201 from the Children's National Hospital (CNH) cohort.

(**B**) Volcano plot of H3K27me3 sites (X-axis, Log_2 fold change between ONC201-treated / untreated H3K27M-DMGs) plotted against -Log10 false discovery rate (FDR). We detected 360 autosomal sites that gained H3K27me3 and 85 autosomal sites that showed decreased H3K27me3 enrichment.

(**C**) Autosomal sites that gained H3K27me3 from **Supplementary Fig. S14B** were compared with H3K27me3-enriched regions in IDH1 mutant gliomas (n=6) and were found to have no overlap. Data for IDH1 mutant gliomas derived from Wu *et al.* (2020).

FIGURE S14

A

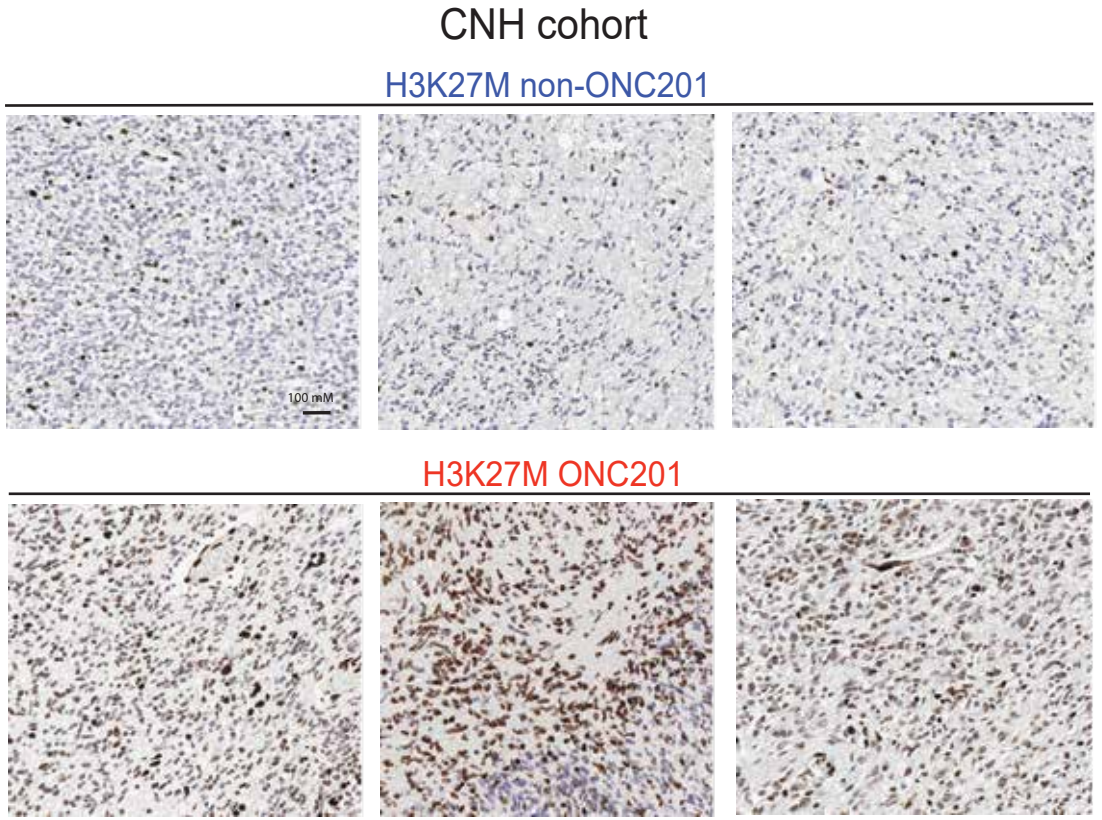

B

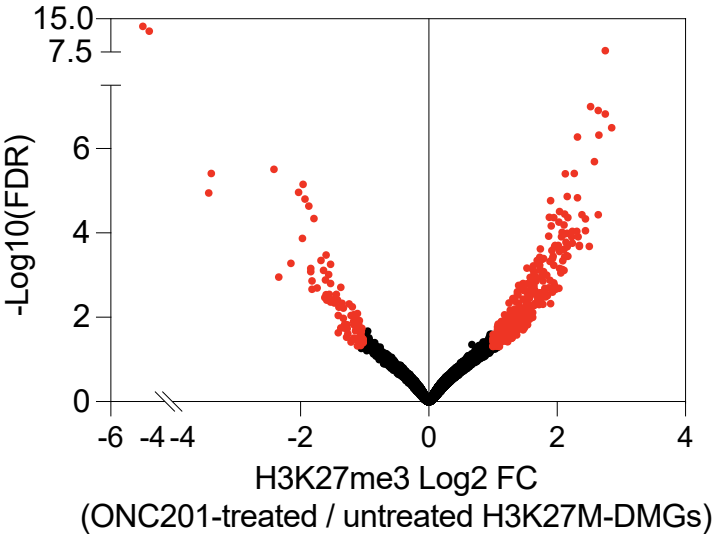

85 autosomal sites with decreased H3K27me3

360 autosomal sites with increased H3K27me3

C

Sites with increased H3K27me3 in IDH1 R132H gliomas (*n*=6)
Wu *et al*. (2020) *Nat. Commun*
GSE 121719

H3K27me3 increase sites
ONC201-treated (*n*=2) / non-ONC201 (*n*=2)
H3K27M-DMGs

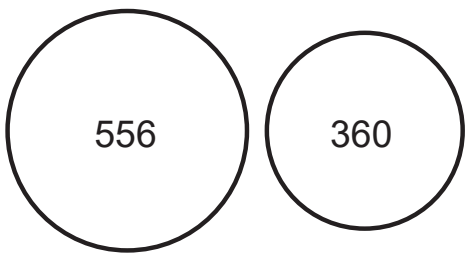

Fig. S15. ONC201 does not cause hypermethylation leading to a glioma CpG island methylator phenotype.

(**A**) Hierarchical clustering of H3K27M-DMGs and lower-grade IDH-mutant gliomas with a G-CIMP phenotype based on methylation values. The heatmap displays 1,000 CpG probes with the highest variance across all samples. *Methylation class*: IDH low-grade (blue) and H3K27M-DMG (red). *Therapy*: ONC201 (yellow) and other (gray). *CpG island status*: yes (green) and no (white).

(**B**) Principal components derived from highly variable (S.D. >0.2) CpG sites showing ONC201-treated H3K27M-DMGs (white), untreated H3K27M-DMG controls (red), and lower-grade IDH-mutant gliomas with a G-CIMP phenotype (blue).

(**C**) Average DNA methylation values for highly variable CpG probes (S.D. >0.2) located within CpG islands for ONC201-treated H3K27M-DMGs (yellow), untreated H3K27M-DMG controls (gray), and lower-grade IDH-mutant gliomas (blue). Only sites that are hypermethylated in lower-grade IDH-mutant gliomas relative to ONC201-treated or untreated H3K27M-DMG controls are shown.

FIGURE S15

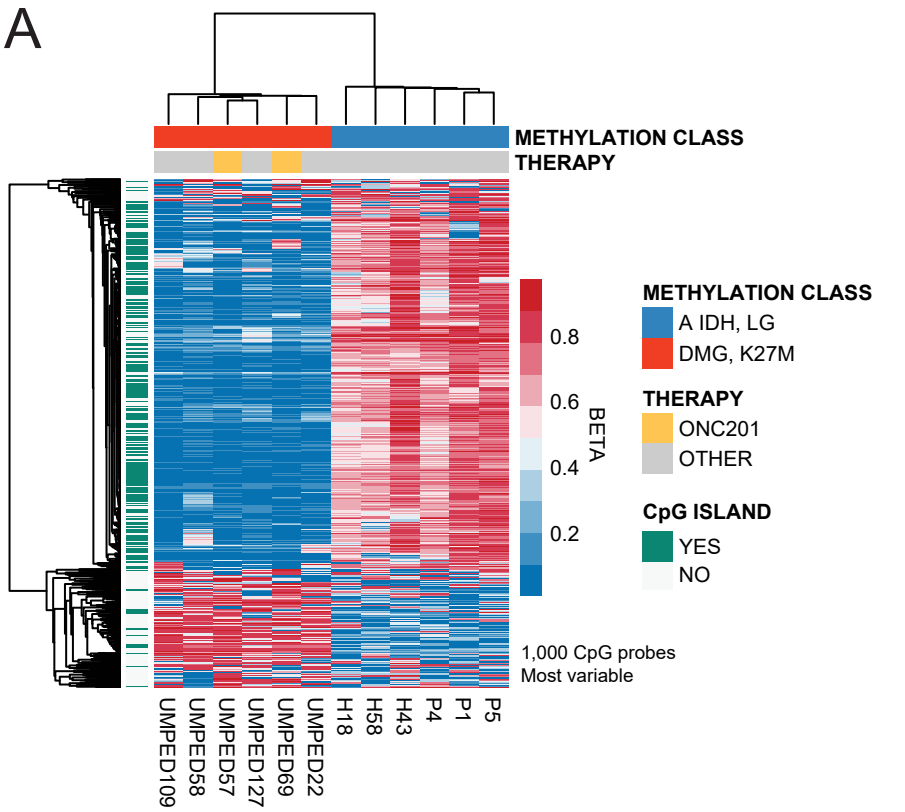

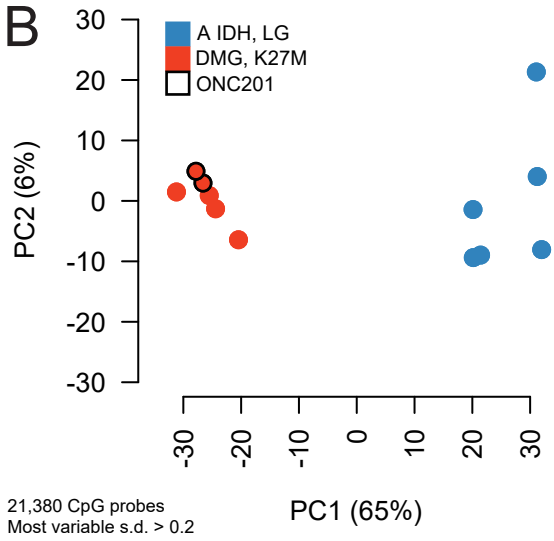

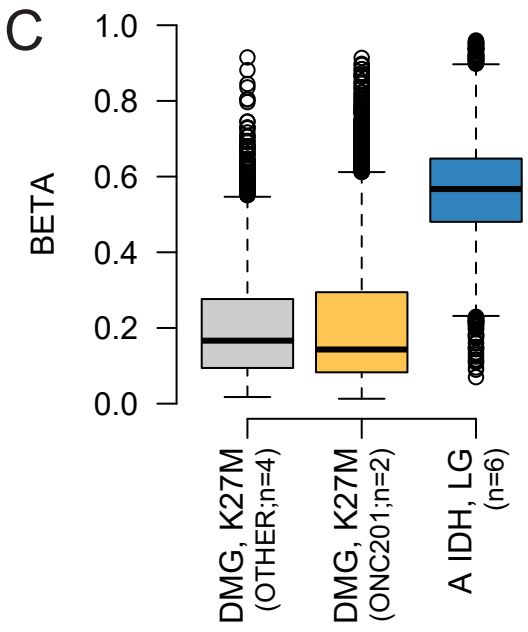

5,667 CpG probes
Most variable s.d. > 0.2
b(A IDH, LG) > b(DMG, K27M)
CpG islands